

MINISTRY OF EDUCATION AND SCIENCE OF THE REPUBLIC OF
KAZAKHSTAN

Kazakh National Research Technical University named after K.I. Satpayev

Institute of Geology, Oil and Mining

Department of Oil, Gas and Ore Geophysics

Uvakova Saule Karimovna

The application of methods of the dynamic interpretation and seismic inversion in the
study of Permian-Triassic sediments of the Pre-Caspian basin

DIPLOMA WORK

Specialty 5B070600 – Geology and exploration of mineral deposits

Almaty 2020

MINISTRY OF EDUCATION AND SCIENCE OF THE REPUBLIC OF
KAZAKHSTAN

Kazakh National Research Technical University named after K.I. Satpayev

Institute of Geology, Oil and Mining

Department of Oil, Gas and Ore Geophysics

ADMITTED TO DEFENCE

Head of the Department of
Geophysics

Doctor of geol.-miner. sciences,
professor



Abetov A.E.

“ ” _____ 2020y.

DIPLOMA WORK

Topic: “The application of methods of the dynamic interpretation and seismic inversion in the study of Permian-Triassic sediments of the Pre-Caspian basin”

Specialty 5B070600 – Geology and exploration of mineral deposits

Done by

Uvakova Saule

Scientific supervisor
PhD, Associate professor



Akhmetzhanov A.Zh.

“ ” _____ 2020y.

Almaty 2020

MINISTRY OF EDUCATION AND SCIENCE OF THE REPUBLIC OF
KAZAKHSTAN

Kazakh National Research Technical University named after K.I. Satpayev

Institute of Geology, Oil and Mining

Department of Oil, Gas and Ore Geophysics

Specialty 5B070600 – Geology and exploration of mineral deposits

APPROVED BY

Head of the Department of
Geophysics

Doctor of geol.-miner. sciences,
professor



Abetov A.E.

“ _____ ” _____ 2020y.

THE TASK

to complete the diploma work

Student Uvakova Saule Karimovna

Topic: “The application of methods of the dynamic interpretation and seismic inversion in the study of Permian-Triassic sediments of the Pre-Caspian basin”

Approved by order of the Rector of the University №762–b from "27" January 2020y.

Submission deadline of the completed work " __ " _____ 2020y.

Initial data for the diploma work: were selected during the completion of industrial practice

Summary of the diploma work:

- a) General information about the area of Saigak deposit (geological-geophysical study, tectonics, stratigraphy, presence of oil and gas)
- b) Analysis of geological and geophysical data in the area of deposit
- c) Processing of seismic materials
- d) Interpretation of geological and geophysical materials

The list of graphic material: are presented ___ slides of presentation work

Recommended main literature: «Prospects for the oil and gas potential of the south-eastern side of the Caspian depression», «The deep structure and mineral resources of Kazakhstan».

GRAPH
of the diploma work preparation

Section Names, list of issues under development	Submission deadline to scientific supervisor	Notes
Geological-geophysical study. Presence of oil and gas		
Analysis of geological and geophysical data in the area of deposit		
Processing of seismic materials		
Interpretation of geological and geophysical materials		

Signatures

of the consultants and standard controller for the completed diploma work with an indication of the sections of work related to them

Section names	Consultants, name, patronymic, surname (academic degree, title)	Date of signing	Signature
Geological-geophysical study. Presence of oil and gas	Akhmetzhanov A.Zh. PhD, Associate professor		
Analysis of geological and geophysical data in the area of deposit	Akhmetzhanov A.Zh. PhD, Associate professor		
Processing and interpretation of geological and geophysical materials	Akhmetzhanov A.Zh. PhD, Associate professor		
Standard controller	Aliakbar M.M.		

Scientific supervisor

signature

Akhmetzhanov A.Zh.

The student fulfilling the task

signature

Uvakova S.K.

Date

" ____ " _____ 2020y.

ABSTRACT

To the diploma work «The application of methods of the dynamic interpretation and seismic inversion in the study of Permian-Triassic sediments of the Pre-Caspian basin»

The following work is composed of the introduction part, 6 chapters, conclusion and list of references.

This paper provides information on the geological and geophysical study of the area, briefly describes the geological structure with the provision of information about stratigraphy, tectonics and oil and gas potential.

Within the Pre-Caspian region, among the suprasalt deposits, the Permian-Triassic reservoirs are the least studied. In the early 2000s, sedimentation deposits were identified and classified in the Middle Triassic sediments on the Sagiz blocks, several small deposits were discovered in lithologically shielded deposits of the Upper Permian. However, the inconsistency of these sediments over the area, as well as low values of porosity, make the efficiency of exploration harder.

Using the example of the Saigak deposit, was developed a methodology for separating the Permian and Triassic sediments using the methods of dynamic interpretation and seismic inversion.

During the stages of processing and interpretation, was used the software of the "Paradigm" company.

3rd chapter is devoted to the analysis of geophysical data on the area of the Saigak deposit, which describes in detail field seismic data and well-logging data. Meanwhile chapter 4 represents the processing of seismic materials, whereas 5th chapter is all about the interpretation of geological and geophysical materials.

The Conclusion illustrates the results of the analysis of the obtained dynamic interpretation data, displays the benefits of application of dynamic interpretation methods.

АННОТАЦИЯ

К дипломной работе «Использование методов динамической интерпретации и сейсмической инверсии при изучении отложений пермского триаса Прикаспийской впадины»

Работа состоит из введения, 6 глав, заключения и списка использованной литературы.

В данной работе приводятся сведения о геолого-геофизической изученности района, кратко описывается геологическое строение с предоставлением сведений о стратиграфии, тектонике и нефтегазоносности.

В пределах Прикаспия из надсолевых отложений пермско-триасовые коллектора являются наименее изученными. В начале 2000-х годов были выделены и классифицированы седиментационные залежи в отложениях среднего триаса на блоках Сагиз, открыты несколько мелких месторождений в литологически экранированных залежах верхней перми. Однако невыдержанность этих отложений по площади, а также низкие значения пористости затрудняют эффективность разведки.

На примере месторождения Сайгак были отработана методика расчленения пермских и триасовых залежей с использованием методов динамической интерпретации и сейсмической инверсии.

При обработке и интерпретации использовалось программное обеспечение компании "Paradigm".

3 глава посвящена анализу геофизических данных по площади месторождения Сайгак, где подробно описаны данные полевой сейсморазведки и данные ГИС. В то время как 4 глава представляет собой обработку сейсмических материалов, а 5 глава интерпретацию геолого-геофизических материалов.

В Заключении представлены выводы по результатам анализа полученных данных динамической интерпретации, показаны преимущества использования методов динамической интерпретации.

АҢДАТПА

Дипломдық жұмысқа «Прикаспий ойпатының пермь-триас шөгінділерін зерттеуде динамикалық интерпретация және сейсмикалық инверсия әдістерін қолдану»

Жұмыс кіріспеден, 6 тараудан, қорытындыдан және пайдаланылған әдебиеттер тізімінен тұрады.

Бұл жұмыста аймақтың геологиялық-геофизикалық зерттеуі туралы ақпарат берілген, геологиялық құрылым қысқаша сипатталып, стратиграфия, тектоника және мұнай-газ әлеуеті туралы ақпарат берілді.

Прикаспий маңында тұзүсті кен орындарынан пермь-триас коллекторлары ең аз зерттелген. 2000 жылдардың басында Сағыз блоктарындағы орта триас шөгінділерінде шөгінділер анықталды және жіктелді, жоғарғы пермияның литологиялық қорғалған шөгінділерінде бірнеше ұсақ кен орындар ашылды. Алайда бұл кен орындарының аудан бойынша сәйкессіздігі, сонымен қатар кеуектіліктің төмен мәні барлау жұмыстарын қиындатады.

Сайгак кен орны мысалын қолдана отырып, динамикалық интерпретация және сейсмикалық инверсия әдістерін қолдана отырып, пермиялық және триас шөгінділерін бөлу әдістемесі жасалды.

Өңдеу және интерпретация кезінде "Paradigm" компаниясының бағдарламалық жасақтамасы қолданылды.

3-тарау Сайгак кен орны ауданында геофизикалық деректерді талдауға арналған, онда сейсмикалық және ГИС мәліметтері толық сипатталған. 4 тарауда - сейсмикалық материалдарды өңдеу туралы жазылған, ал 5-тарауда - геологиялық және геофизикалық материалдарды интерпретациялау барысы сипатталады.

Қорытынды бөлімінде алынған динамикалық интерпретация мәліметтерін талдау қорытындыларын ұсынады, динамикалық интерпретация әдістерін қолданудың артықшылықтарын көрсетеді.

CONTENTS

Introduction	11
1 Basis of the diploma work	12
2 General information about the area of work	13
2.1 General information about the area of Saigak deposit	13
2.2 Geological and geophysical knowledge	14
2.3. Lithological and stratigraphic characteristics	16
2.4 Tectonics	19
2.5 Presence of oil and gas	20
3 Analysis of geological and geophysical data in the area of the deposit	25
3.1 Field seismic data	25
3.2 Well-logging data	27
4 Processing of seismic materials	29
4.1 Initial data analysis	29
4.2 Testing procedures and parameters of processing	29
4.2.1 Testing the parameters of the main processing procedures before summation	29
4.2.2 Amplitude recovery	30
4.2.3 Suppression of noise in the zone of close distances	30
4.2.4 Trace editing. Suppression of random noise. Lift-technology	30
4.2.5 Suppression of the surface waves	31
4.2.6 Minimum-phase conversion	31
4.2.7 Deconvolution	31
4.2.8 Suppression of the noise after deconvolution	32
4.2.9 Surface-matched amplitude correction	32
4.2.10 Refracted statics	33
4.2.11 Correction of static corrections	33
4.2.12 Subtraction of multiple waves	33
4.2.13 Residual statics and increase of signal coherence	34
4.2.14 Migration in the time domain	34
4.3 Testing parameters after the summation	35
4.3.1 Increase of signal/noise ratio	35
4.3.2 Suppression of the regular noise. FK-filtration	35
4.3.3 Increase of the signal coherence	35
4.3.4 Bandpass filtering	36
4.4 Processing graph before and after summation	36
4.4.1 Processing graph before summation	36
4.4.2 Processing graph after summation	37
4.5 Depth migration before summation (PreSDM)	38
4.5.1 Goals and objectives of the deep migration before summation	38

4.5.2 Initial data loading	38
4.5.3 Construction of a velocity model	38
4.5.4 Testing parameters of depth migration (PreSDM)	40
4.5.5 Residual analysis and post-migration processing	40
4.5.6 Wells	41
4.6 Conclusion of the Processing part	49
5 Interpretation of geological and geophysical materials	51
5.1 Structural interpretation	51
5.1.1 Stratification of reflecting horizons	51
5.2 Data interpretation of the wells	52
5.2.1 Clay content calculation	53
5.2.2 The calculation of the coefficient of porosity	53
5.2.3 Saturation calculation	55
5.2.4 Acoustic impedance	59
5.2.5 Lithofacial analysis	59
5.3 Seismic inversion	60
5.4 Coherence	70
5.5 Seismic facial analysis	72
6 Analysis of the dynamic interpretation results	76
Conclusion	83
List of references	

INTRODUCTION

The work on this diploma work began in the early 2019 and continued this summer as a part of an internship at "Saigak Kazakhstan B.V." company. The processing and interpretation of geophysical data was carried out in the city of Almaty by the company "Seismic Geophysical Services".

The author was given the opportunity to trace all the stages of processing and interpretation of seismic data, and also had the chance to actively participate in conducting the dynamic analysis using methods of seismic stratigraphy and seismic inversion.

During the processing and interpretation, the software of the "Paradigm" company was used.

Using the example of the Saigak deposit, was developed a methodology for separating the Permian and Triassic sediments using the methods of dynamic interpretation and seismic inversion.

The following work provides information on the geological and geophysical study of the area, briefly describes the geological structure with the provision of information about stratigraphy, tectonics and oil and gas potential.

Within the Pre-Caspian region, among the suprasalt deposits, the Permian-Triassic reservoirs are the least studied. In the early 2000s, sedimentation deposits were identified and classified in the Middle Triassic sediments on the Sagiz blocks, several small deposits were discovered in lithologically shielded deposits of the Upper Permian. However, the inconsistency of these sediments over the area, as well as low values of porosity, make the efficiency of exploration harder.

1 Basis of the diploma work

Within the Pre-Caspian area, among the suprasalt sediments, the Permian-Triassic reservoirs are the least studied. In the early 2000s, sedimentation deposits were identified and classified in the sediments of Middle Triassic on the Sagiz blocks, several small deposits were discovered in lithologically shielded deposits of the Upper Permian. However, the discontinuity of these sediments over the area, as well as the low values of porosity, do make the efficiency of exploration more difficult.

Using the example of the Saigak deposit, the author tried to analyze the effectiveness of processing methods and interpretation of seismic data on Permian-Triassic sediments using dynamic interpretation and seismic inversion methods.

This work represents the results of a complex interpretation of the 3D MCDP seismic survey obtained in 1998-1999, together with the results of drilling works within the deposit.

Seismic studies were carried out with the aim of detailing the structural-tectonic model of Permian - Triassic suprasalt sediments, clarifying the contours of oil deposits in the Saigak deposit. The work accomplished to clarify the geological model, including high-precision processing of 3D data, their structural and dynamic reinterpretation, clarified the structure of the Saigak deposit and confirmed its prospects, in particular, were identified zones of reservoir development within the arch part of the structure.

The main objective of the research was to – determine the location of the prospecting and exploration wells for oil and gas within the mining allotment of the company “Saigak Kazakhstan B.V.” based on the reprocessing of 3D seismic data according to modern graphs of processing systems, structural reinterpretation and interpretation of the dynamic processing of seismic materials.

Based on seismic data, a structural interpretation was performed to clarify the geological structure of the area under consideration in Permian and Triassic subsalt sediment complexes, with the link to reflecting horizons to geological data based on interpretation of well-logging materials.

The procedures for the dynamic processing and interpretation of seismic data were performed, those are - seismic inversion and coherence. The results are compared with well-logging interpretation data.

Based on the results of the performed work, were determined the points for exploratory drilling in the Permian and Triassic rock complexes within the mining allotment of the Saigak deposit.

The total volume of seismic materials for interpretation over the reporting area amounted to 32 km² of CDP 3D, Well-logging data were interpreted - for 8 wells.

2 General information about the area of work

2.1 General information about the area of Saigak deposit

The Saigak oil deposit is located in the southeastern part of the Aktobe region. The nearest settlements are the Shubarkuduk railway station, located in 15 km northwest of the deposit, the regional center of Aktyubinsk city is 175 km from the area of the Saigak deposit (Figure 2.1).

In the orographic sense, the territory of the deposit is a plain crossed by small rivers (mainly drying up), dry channels and ravines.

The water in all rivers and streams is fresh, of good quality. Water supply of settlements which are existing on the territory is carried out from rivers, lakes and wells. For technical needs, Upper Cretaceous sediment water can be used.



Figure 2.1 – Overview map of the work area on a scale of 1:1 000 000

According to climatic conditions, the area of the deposit belongs to the semi-desert zone. The climate is sharply continental with temperature fluctuations: from plus 40C in the summer to minus 38C in the winter, rainfalls are in the spring, autumn and winter. The average amount of annual rainfall rarely exceeds 200 mm. The thickness of the snow cover is up to 0.5 m, the depth of soil freezing reaches 2.0 m. In winter, spring and autumn, winds of the east and north-east direction dominate on the territory of the deposit, their average velocity in January and February - is 5 m / s, and the annual wind velocity is not more than 4.0 m/s.

The plant world is represented by grasses, only on the slopes of large ravines and along river banks can be met a thicket of shrubs. The hydrographic network in the described territory is developed very poorly.

The fauna is relatively poor: there are wolves, foxes and saiga, a lot of rodents - ground squirrels, jerboas, ferrets. Among the birds there are eagles, ducks, partridges. Among the reptiles - snakes, cottonmouth, steppe vipers, as well as phalanges, scorpions and tarantulas are also found.

From an economic point of view, the deposit area is favorable for development: nearby are Kenkiyaks koye, Zhanazholskoye and other oil and gas deposits, there are water sources, raw material bases of construction materials.

2.2 Geological and geophysical knowledge

The Saigak deposit is located within the Temir Licensed Block.

In the mid 30-ies of the last century, in order to study the geological structure of this site, a large amount of geological exploration was performed. Based on the results of the first geological and gravimetric surveys, regional geological and gravimetric maps were constructed.

This section provides brief information about the methodology and results of geophysical surveys directly at the deposit and in the neighboring areas of the Temir block.

Until 1992, seismic exploration work on the Temir block was mainly focused on the search and exploration of oil and gas deposits in subsalt sediments of the Temir carbonate platform. Many subsalt structures have been identified, large of which were subsequently tested by drilling. Oil and gas deposits were not discovered during this period. In the subsequent goal of prospecting and exploration works, suprasalt Upper Permian and Triassic sediments were planned to be identified. The methodology and technique for conducting field seismic surveys was reoriented to this complex of sediments. Interpretation of the suprasalt sediments over the entire area illustrated that the main potentially promising objects are strata of the Triassic and Upper Permian sandstones.

In the year of 1994, «JekaPrakla» company carried out 2D seismic surveys on suprasalt Triassic and Upper Permian sediments. Based on the materials of these

works, structural maps were constructed on the roof of the Triassic sediments and a domed Saigak uplift was revealed. In 1995, an exploratory drilling begun on the area of Saigak. As a result of drilling exploratory well 1 in the area, an oil inflow of 128 m³/day was obtained at a 32 mm pipe when testing the Upper Permian sediments (interval 1924-1944 m).

In 1998, directly at the Saigak deposit, seismic surveys in 3D modification were carried out by Shell Temir Petroleum Development BV using a vibration source of excitation of elastic vibrations. Based on the results of the work, the geological structure of the deposit was clarified. Were identified eight reflecting horizons, which are stratigraphically associated with sediments of the Upper Permian and Lower Triassic. Structural maps were built across all horizons. Based on these works, a project for drilling an exploratory well was drawn up.

In 2001-2002, «MaerskOilKazakhstanGmbH» company carried out a reinterpretation of seismic data obtained in 1998, on the basis of which an updated model of the geological structure of the deposit was created, according to which there is a mismatch in the structural plans of uplift along the Upper Permian and Triassic productive horizons. The arched part of the uplift along the Triassic is located northeast of well 2, and the arched part of the uplift along Permian is shifting to the bottom hole of the well 6. With depth, the contrast of the structure increases.

Consequently, according to the obtained 3D seismic data, a large complex of work was performed on processing and reprocessing of seismic data using various technologies in order to obtain the most reliable picture of the geological structure of the deposit. Both domestic and foreign geophysical companies took a part in the processing of the material.

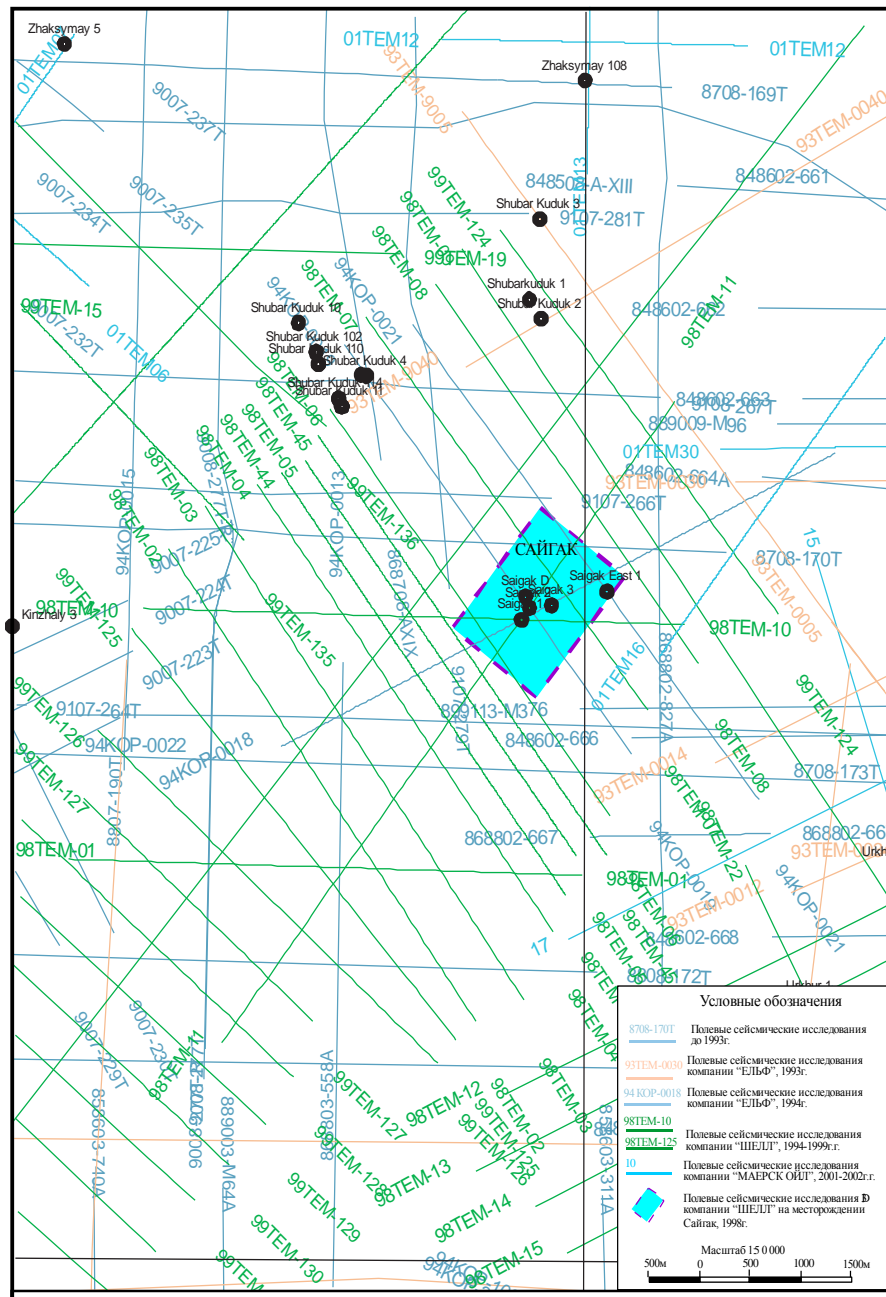


Figure 2.2 – Fragment of a map of seismic exploration of the Temir block

2.3 Lithological and stratigraphic characteristics

Within the Saigak deposit, as a result of drilling exploratory, estimated and production wells, was discovered a layer of Lower Permian-Quaternary sediments with a maximum thickness of 3030 m (well Saigak-2).

The stratigraphic separation of the cross-sections of wells was carried out using a Well-logging complex based on microfaunistic and palynological analyzes, as well as lithological and petrographic description of core and sludge.

Below is a brief characterization of the stratigraphic complexes discovered in the deposit.

Paleozoic era - Pz

Within the area, Paleozoic sediments are distinguished in the volume of the lower and upper Permian.

Permian system – P

Lower epoch - P₁

Open sediments of the Lower Permian are represented by the Kungurian stage.

Kungurian stage-P_{1kg}

The sediments of the Kungurian stage are represented by halogen-sulfate rocks of gray and dark-gray colour. In the cross-section, along with rock-salt and anhydrites, are found interlayers of mudstones and sandstones. The open maximum thickness in well 6 is 237 m.

Upper epoch - P₂

Upper Permian sediments are represented by two stages: Kazanian and Tatarian.

Kazanian stage – P_{2kz}

The sediments of the Kazanian stage opened in well 2 are represented by interbedded dense bright-coloured sandstones, clays and gray marls with an open thickness of up to 67 m in well 6.

Tatarian stage – P_{2t}

The sediments of the Tatarian stage are lithologically represented by sandstones, siltstones and clays.

Sandstones are polymictic, medium-grained and heterogeneously-grained, gray, brown and light-brown, calcareous.

Siltstones of brownish-gray, dull-brown colour, calcareous, sometimes clayey, grains of carbonized vegetation are noted.

The clays are bright-coloured, massive and lumpy, with a high content of carbonates.

In the sediments of the Tatarian stage, 11 horizons were distinguished (P-0 to P-10), of which the productive are: P-1 – P-4; P-6 – P-10.

In the roof of the Tatarian stage, the water-bearing horizon P-0 (aquifer) is distinguished. Its maximum thickness is 75 m in well 8.

Horizon P-5 is also completely water-saturated; no oil-saturated layers were identified in its cross-section. Maximum open thickness is 123 m in the borehole 8.

The opened thickness of the Tatarian stage reaches from 43 m (well 4) to 1201 m (well 1bs).

Mesozoic group-Mz

Mesozoic sediments in the deposit are represented by the Triassic, Jurassic and Cretaceous systems.

Triassic system-T

Triassic sediments belong to the lower epoch.

Lower Triassic-T₁

Opened sediments of the Lower Triassic are represented by the Yershovian stage (local suite).

The Lower Triassic sediments with angular disagreement lie on the blurred surface of the Upper Permian sediments and are lithologically represented by an alternation of brownish-brown, reddish-brown and greenish-gray clays, polymictic sandstones, various-grained sands, strong conglomerates and calcareous mudstones. The open thickness of these sediments varies from 1254 m (well 4) to 1486 m (well 3).

In the lower part of the Triassic sediments, productive horizons T-1 and T-2 are distinguished.

Jurassic system - J

Jurassic sediments occur with stratigraphic disagreement on the blurred surface of the Lower Triassic sediments.

They are represented by the lower and middle epochs, which are lithologically composed of gray, dark gray, and dense sandstones.

Cretaceous system - K

Cretaceous sediments occur with stratigraphic disagreement on the blurred surface of the Middle Jurassic sediments, represented by the lower and upper epochs.

Cretaceous sediments are lithologically represented by gray sandstones, greenish-gray clays, marls with interlayers of conglomerates.

The uncovered strata of the Jurassic-Cretaceous sediments varies from 360 m (well 1) to 720 m (well 9).

Quaternary system - Q

Quaternary sediments everywhere overlap sediments of the Upper Cretaceous, represented by loam and sandy loam. Thickness 2-3 m.

2.4 Tectonics

The Pre-Caspian basin is situated on the southeastern edge of the East European platform. In the west and north it is articulated along the system of peripheral ledges with the indicated platform, in the east it is limited by the folded structures of the Ural and Mugodzhär. The South Emba fault separates the basin in the southeast from the North-Ustyurt massif. In the south-west, the borderline extends beneath the Donbass-Astrakhan integument-thrust zone. Within the limits of the latter, the Upper Paleozoic fold-thrust strata of the Karpinsky ridge are pushed by 35-80 km onto the Paleozoic sediments of the Pre-Caspian basin.

According to the crystalline basement, the Pre-Caspian basin is a large asymmetric negative structure. According to the structural map of the basement surface edited by L. M. Rovnin and S. E. Chakabaev, the largest structural zone of the southeastern side of the Pre-Caspian basin is the Aktobe-Astrakhan system of uplifts, a giant half-ring enveloping the central part of the Pre-Caspian basin. Within

this structural zone, a number of bendings, ledges, and uplifts stand out. The main structural element of the Aktobe-Astrakhan zone, located within the research area, is the Temir uplift, complicated by the Enbek and Aransai ledges.

The crystalline basement is everywhere covered by a sedimentary cover. The total thickness of sedimentary cover deposits in the central part of the basin can reach 20–25 km. Here, the thickness of the subsalt complex also reaches the maximum values (17 km), which in the south is reduced to 7-10 km. The northern and eastern sides of the basin are characterized by minimal (about 5 km) thicknesses of subsalt deposits. The thickness of the suprasalt complex varies from 2-4 km along the frame of the depression till 5-6 km in the central part [2].

The Saigak deposit is located within the Shubarkuduk uplift of the Eastern near edge zone part of the Caspian depression (figure 2.3).

The deposit is confined to the salt stage complicating the northwest slope of the Saigak dome.

Salt movements play a special role; they mainly determine the structure of the suprasalt part of the cross-section. The vertical and horizontal flow of salt depended to a large extent on the amount of precipitation overlapping it. The movement of salt strata formed the local uplifts and faults in the Mesocenozoic sediments, confined to the tops of salt domes.

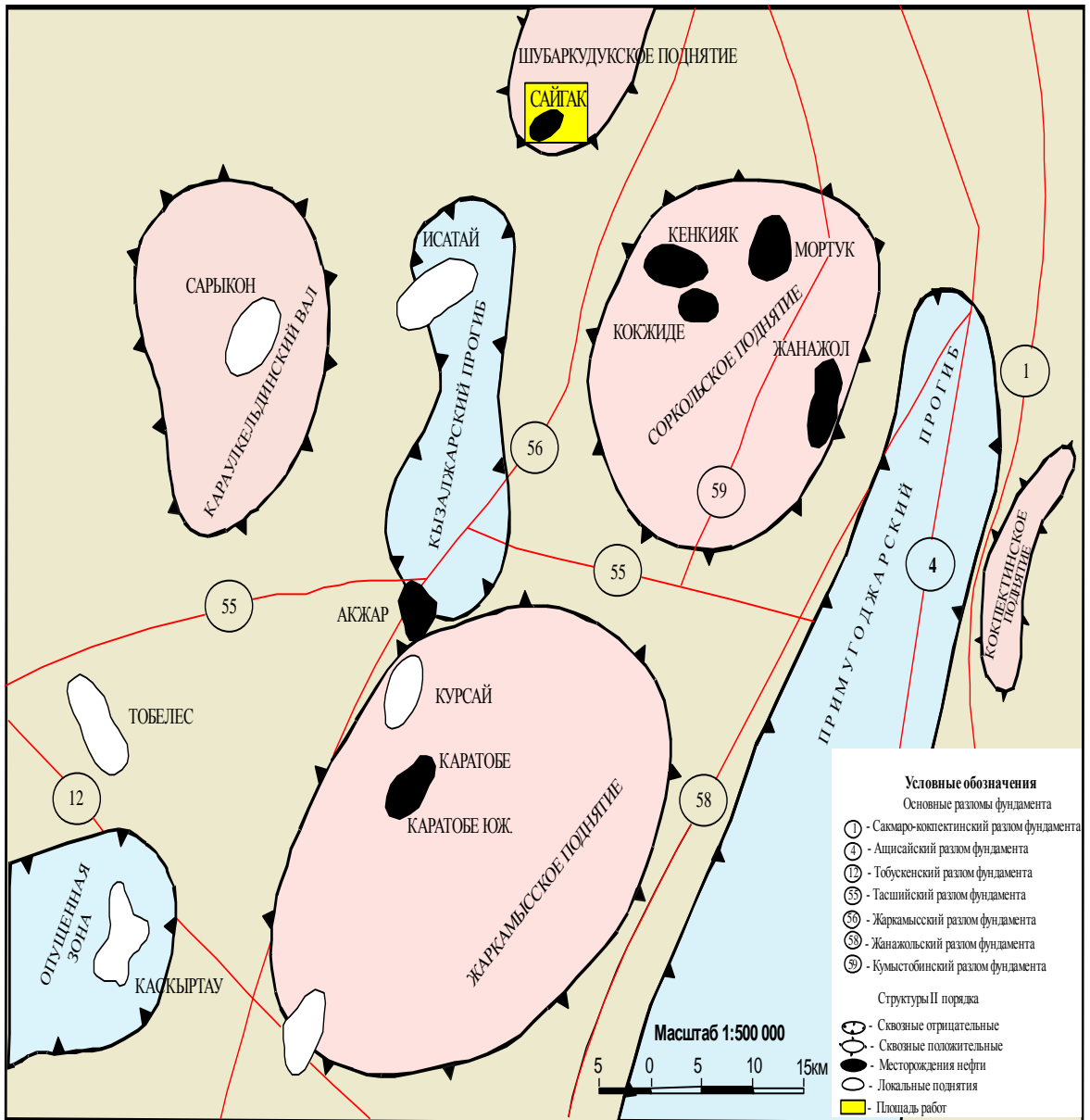


Figure 2.3 – Eastern part of the Precaspian basin, Scheme of tectonic zoning of the suprasalt rock complex

2.5 Presence of oil and gas

The Pre-Caspian oil and gas province unites a number of oil and gas areas and regions characterized by different geological structures and the distribution of oil and gas complexes by the cross-section and area. The tectonic factor had a decisive impact on the formation of hydrocarbon accumulations; therefore, the boundaries of the oil and gas geological zoning elements in the vast majority of cases coincide with the contours of tectonic elements.

In terms of oil and gas geological zoning, the Saigak deposit belongs to the Borzher-Akzharsky highly promising region of the Embinsk-Aktobe oil and gas region, which is one of the most promising in the eastern part of the Caspian basin (G.E.A. Aizenshtadt, A.I. Dimakov and etc., 1988; Kh. B. Abilhasimov, 2009). Borzher-Akzharsky highly promising area is confined to the tectonic step of the same name, complicated by shafts and local uplifts. The oil presence prospects of the eastern side of the Caspian depression have been proved by the discovery of industrial oil deposits Kenkiyak, Kumsay, Laktybai, Karatyube, Zhanatan, Zhaksymay, Akzhar, East Akzhar and etc. On number of rows of salt domes, oil presence signs are noted and their further study is conducted. Industrial oil content and oil features in the above-listed structures are established in the Upper Permian, Triassic, Jurassic and Lower Cretaceous sediments.

In the Saigak deposit under consideration, according to the results of well testing and assessment of the saturation characterization of the reservoirs, according to the Well-logging data in the cross-section of the Permian-Triassic sediments, 11 productive horizons and associated with them oil deposits were established, of which 2 deposits are associated with the Triassic sediments, and 9 - with the Upper Permian. Reservoirs are polymictic sandstones with a complex structure of the void space. Fluid-resistances are interformational clay packs, which are separating productive horizons. As lateral fluid-resistances we take lithological and tectonic screens.

The filtration-capacitive properties of reservoir-rocks by core have been studied in the productive horizons T-1, T-2, P-1, P-2, P-3, P-5.

The allocation of reservoir-formation in the cross-section of each well was carried out according to the materials of field-geophysical studies.

Productive horizon testing results

The **T-1 horizon** was discovered by all drilled wells. Productivity of the horizon has been proven by testing wells 1, 2, 3, 4, and 7.

In well 6, according to the well-logging data, 5 oil-saturated reservoirs were identified, the testing of which was not carried out. According to INNL data at the time of the study (01.12.12y), the strata were characterized as weakly oil-saturated, K_{oilgas} within 30%.

In well 1, after conducting INNL studies in a cased borehole to determine the current saturation from 17.03.13, the strata are partially flooded.

The porosity coefficient according to core analyzes varies from 0.139 to 0.280 unit fraction, the average weighted value is 0.217 unit fraction. According to the Well-logging data, the porosity coefficient is in the range 0.15-0.2 unit fraction.

The **T-2 horizon** was discovered by all drilled wells. Horizon productivity has been proved by joint testing and obtaining oil and gas inflows in wells 2, 3, 4. In wells 7, 8 and 9, the formations are water-saturated.

In well 1, according to INNL studies (dated 17.03.13 y.), all oil-saturated formations are flooded.

In well 6, according to the Well-logging data, in the horizon interval three oil-saturated formations were identified in the intervals 1937.1-1940.6, 1941.8-1942.9 and 1946.3-1948.2 m, the formations were not tested. After INNLL studies to determine the current saturation of $K_{oil/gas}$ formations - 35.5, 49.4, 41%, respectively. Formations are recommended for testing.

The porosity coefficient according to core analyzes varies from 0.141 to 0.262 unit fraction, the average weighted value is 0.197 unit fraction. According to the Well-logging data, the porosity coefficient is in the range 0.14-0.2 unit fraction.

The **P-1 horizon** was discovered by all drilled wells, with the exception of well 4. In wells 1, 6, 2, and 9, the horizon is with the product. The horizon was tested in wells 1, 2 and 6.

In well 1, according to INNLL research, the perforated formation in the interval 1873-1878 m is partially flooded.

In well 9, testing of the P-1 horizon was not carried out. According to the research conducted by INNLL to determine the current saturation from 12.03.19 y., the formation in the interval 1982.3-1986.1 m with good saturation, $K_{oil/gas}$ up to 63%. The formation in the interval 1996.1-2000.7 m is slightly oil-saturated, $K_{oil/gas}$ is up to 36%. The formation in the interval 2015.8-2017.6 m is slightly oil-saturated, $K_{oil/gas}$ is up to 45%. Formations are recommended for testing.

In wells 3, 7 and 8, the formations of the horizon are water-saturated.

The porosity coefficient according to core analyzes varies from 0.165 to 0.233 unit fraction, the average weighted value is 0.215 unit fraction. According to the Well-logging, the porosity coefficient is in the range of 0.10-0.20 unit fraction.

The **P-2 horizon** was discovered in 1, 2, 3, 6, 7, and 8 wells. In wells 1, 6, 2, and 9, the P-1 horizon with the product was tested in wells 1, 2, and 6.

In the well 1, the non-perforated interval of 1956.6-1957.7 m, according to INNLL data, is watered.

In the well 6, when determining the current saturation according to INNLL research (dated 01.12.12 y.), the perforated formation in the interval 2176-2183.5 m is flooded.

In the well 9, the horizon has not been tested. After the INNLL studies in the cased hole, the formation in the interval 2069.6-2072.6 m with $K_{oil/gas}$ up to 30% - the formation is characterized as slightly oil-saturated.

In wells 3, 7 and 8, the layers of the horizon are water-saturated.

The porosity coefficient according to core analyzes varies from 0.131 to 0.242 unit fraction, the average weighted value is 0.216 unit fraction. According to the Well-logging data, the porosity coefficient is in the range of 0.10-0.20 unit fraction.

The **P-3 horizon** was discovered in 1, 2, 3, 6, 7, and 8 wells. In wells 1 and 6, the horizon with the product was tested in both wells. In well 1, according to INNLL studies, the formations are partially flooded.

In well 6, according to INNL studies, the perforated formations in the total interval 2252.5-2268.5 m are completely flooded. Formations in the range of 2286–2308 m are also completely flooded.

In wells 2, 3, 7, 9, and 8, the formations of the horizon are water-saturated.

The porosity coefficient according to core analyzes varies from 0.140 to 0.239 unit fraction, the average weighted value is 0.191 unit fraction. According to the Well-logging data, the porosity coefficient is in the range of 0.10-0.19 unit fraction.

The **P-4 horizon** was discovered in 1, 2, 6, 9, and 8 wells. In wells 1 and 6, the horizon with the product was tested in both wells. In well 1, according to INNL research, the formations are partially flooded, from a depth of 2082 m all the formations are flooded.

In well 6, in the interval 2331.8-2336.6 m, the formations are characterized as oil-saturated according to INNL data. The formations below are either flooded or with residual saturation.

In wells 2, 9 and 8, the formations of the horizon are water-saturated.

According to the Well-logging data, the porosity coefficient is in the range of 0.08-0.19 unit fraction.

The **P-5 horizon** was discovered in 1, 2, 6, 9, and 8 wells. The horizon is fully water-saturated.

The **P-6 horizon** was discovered in 1, 2, 6, 9, and 8 wells. In wells 1 and 6, the horizon with the product was tested in both wells. In wells 2, 9 and 8, the formations of the horizon are water-saturated.

According to the well-logging, the porosity coefficient varies from 0.08-0.16 unit fraction.

The **P-7 horizon** was discovered in 1, 2, 6, 9 and 8 wells. In the wells 1, 2, 6, 9 reservoirs are with a product. Only in the well 2 strata were tested, oil production rate was 4.8 m³ / day.

Porosity coefficient by the well-logging is in the range of 0.08-0.10 unit fraction.

The **P-8 horizon** was discovered in 1, 2, 6, 9 wells. The strata were tested in well 2.

Porosity **coefficient** by the well-logging is altering from 0.10 unit fraction. When testing well 2, an overflow inflow of oil was obtained with a flow rate of 4.8 m³ / day.

The **P-9 horizon** was discovered in 1, 2, 6, 9 wells. The product is released only in well 2. The reservoir was tested in conjunction with the horizons P-7, P-8.

Porosity coefficient by the well-logging varies from 0.07-0.10 unit fraction.

The **P-10 horizon** was discovered in 1, 2, 6, 9 wells. In the well 1, horizon is without a product. In 2 and 9 wells, the reservoirs were tested. When testing in well 9, was obtained an inflow of oil with a flow rate of 13 m³ / day with a 10 mm branch pipe.

3 Analysis of geological and geophysical data in the area of the deposit

3.1 Field seismic data

The total volume of 3D seismic survey is equal to 32 km², while the full-multiple volume was 27 square kilometers.

The parameters and methodology of the seismic survey are described in the table No. 1.

Table 1 – The parameters and methodology of the seismic survey

№	Name of parameters	Parameters
	Arrangement pattern	
1.	Full multiplicity	30 (60)
2.	Bin size [m x m]	12.5×12.5
3.	The number of receiver lines (RP) in the strip	17
4.	The number of receiver points (RP) on the receiver line (RL)	61
5.	Number of active channels	366 (726)
6.	Step of receiver points (RP) on RL [m]	50
7.	Interval between receiver lines [m]	600
8.	Maximum "shot-receive" removal	3315
9.	Number of shot points on the shot line	144
10.	The step of the shot points (SP) on the shot line (SL) [m]	25
11.	Interval between shot lines (SL) [m].	275
	Parameters of actuation	
1	Total amount of signal actuation points in the shooting area	5429
2.	The method of signal actuation	vibrator
3.	Type of vibrators	Mertz 18 HD
4.	Number of vibrators	4
5.	Amount of accumulations	2
6.	Sweep frequency range	8-70 Hz
7.	Sweep length	12 s
	Parameters of receiving	
1.	Type of seismic receivers	SensorSM 4B
2	Number of seismic receivers per trace	12
3	Length of the grouping base [m].	18,5
	Parameters of registration	
1.	Type of seismic station	I/OSystemTwo
2	Record length; step of discretization	6 s; 2 ms
3	Recording format	SEGD

In the area of the Saigak deposit, the project multiplicity of the seismic exploration work reached 60 only in the north-east and south-west of the area. In the

center of the region, the multiplicity drops to 3 due to poor overlapping of the receiver lines (only 6 channels, i.e. 300m), therefore, the field seismic survey technique is not entirely conditional for processing.

The multiplicity diagram is illustrated in Figure 3.1. The numbers in this figure indicate the coordinates of the survey 3D text application 9.

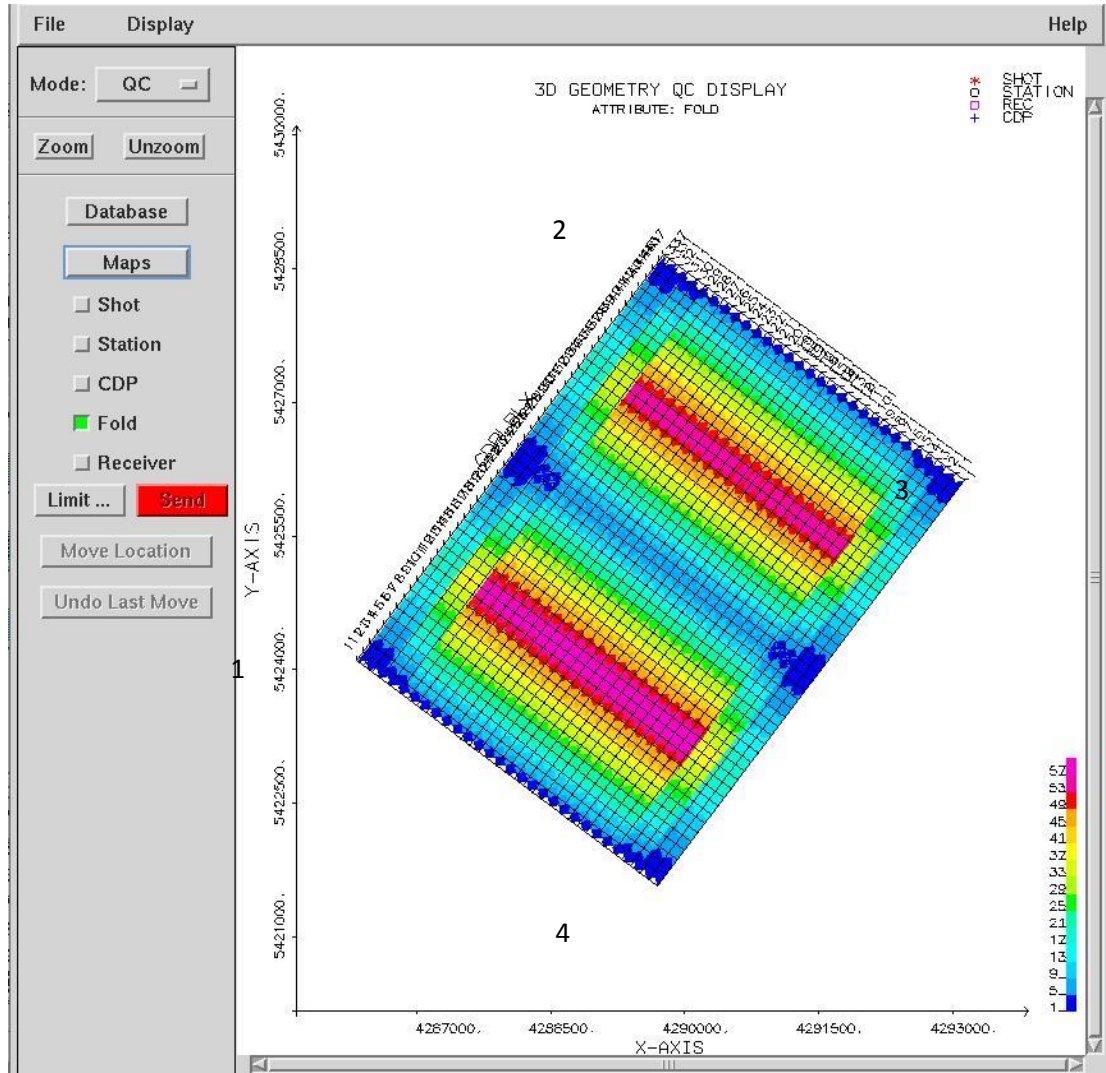


Figure 3.1 – Map of multiplicity of Saigak region

3.2 Well-logging data

A total of 8 wells were drilled at the deposit, there are:
 well 1-search well, in which the industrial inflow of oil was obtained by testing the Upper Permian and Triassic deposits
 wells 2, 3 - exploratory wells,
 wells 4, 6, 7,9 - production wells,
 well 8 - injection well.

Consequently, well 3 was also transformed into an injection well in order to support the pressure in the Triassic horizons.

Based on the materials of the full well-logging complex, a qualitative and quantitative reinterpretation was performed. Rock lithology, total and effective porosity, clay content, oil and gas saturation coefficient were determined.

Reservoirs identified according to well-logging data are represented by sandstones containing clay minerals.

Productive horizons are stratigraphically confined to the Lower Triassic and Upper Permian deposits. Productive of these are T-1, T-2, P-1, P-2, P-4, P-6, P-7, P-8, P-9 and P-10. Horizon P-5 - is represented by water-saturated reservoirs.

Received Well-logging materials in Las format meet the requirements of the “Technical Instructions for conducting geophysical surveys in wells” and technical recommendations for downhole tools. With the exception of the diagrams of natural potentials, depending on the ratio of the electrical resistances of the drilling fluid and formation water, the SP curves in the wells are not differentiated.

Logging works in all wells was carried out by company Schlumberger.

Wellbores 1, 2, 3 – are vertical, wells 4, 6, 7, 8, 9 – are angular directed. Monitoring the spatial position of angular-directional and horizontal wellbores during drilling was carried out by recording inclinometry. These curvatures were taken into account during geological constructions, in determining the location of the well bottom, the absolute elevations of the exposed formations.

For all wells, projections of the wellbore were constructed taking into account inclinometry.

4 Processing of seismic materials

All the processing and analysis of the wave field was carried out using the programs of «Paradigm» JSC. The datum line was accepted during processing +120 m.

4.1 Initial data analysis

The initial material is complicated by irregular and various kinds of regular low-frequency noise, noisy channels.

The variability of near-surface conditions affects the dynamics and tracking of productive horizons. The relief of the area varies between 182 and 260 meters.

The creation of geometry from field SPS-files was accompanied by quality control, by building maps of the location of sources and receivers, as well as checking the conformity of topographic data to the geometry of seismic data.

Since the step of SP is 25 m and the step of RP is 50 m, was required the interpolation of the traces at the shot point and the receiving of the receiver points through 25 m for an even binning step. Thus, the bin size is 12.5×12.5 m, and the multiplicity is increased from 30 to 60. But the field seismic survey technique is not entirely conditional for processing. The multiplicity decreases in the center of the inline till 3 (the receiver lines are overlapped only at 6 channels, which is 300 m). For the correction of statics, flattening of amplitudes, and migration by the initials, such conditions are not entirely satisfactory (edge effect).

4.2 Testing procedures and parameters of processing

In order to select the graph and parameters of the processing procedures, the parameters were tested on the initial and cumulative traces. Before testing, it was completed: data entry, geometry assignment and control, editing of the noisy traces.

4.2.1 Testing the parameters of the main processing procedures before summation

In order to select a processing graph, testing of the procedures for the initial and cumulative traces was carried out. Before testing, it was completed: data entry, geometry assignment and control, editing of the noisy traces. Previously, the sum v1s1 (velocity and statics correction) was obtained from the initial data with AGC and single-channel deconvolution. These velocities and static correction were used for testing. After selecting the parameters, the static correction was recalculated and the velocities specified.

4.2.2 Amplitude recovery

The amplitudes were restored at the preliminary processing stage according to the formula:

$$A=A(i) \times T(i)^N / RL^N$$

where:

A – amplitude for discrete “i” after restoration;

A(i) – amplitude for discrete “i” before recovery;

T(i) – time of discrete “i”;

N – indicator of the degree of amplification function;

RL – length of the trace.

In order to compensate the attenuation, those values were tested N:1.4,1.6, 1.8, 2.0.

Based on the analysis of the test results, the parameter **N = 1.6** was chosen.

4.2.3 Suppression of noise in the zone of close distances

In order to reduce the level of noise at close distances, it was necessary to use the editing procedure in the zone of close traces, such as the use of the Gain program in the zone of internal muting. Noise is suppressed at a given time with a specific suppression coefficient.

The suppression coefficient was tested (dB) 9; 12; 18; 25

Noise suppression was selected in the zone of internal muting with a variable suppression coefficient at distances of 35-79 and variable in time.

4.2.4 Trace editing. Suppression of random noise. Lift-technology

The Ampscal program is used to suppress amplitude anomalies (noisy traces, sound wave, signal distortion caused by surface conditions) and amplitude flattening inside the CSG (common shot gather) seismogram.

The algorithm of this program is that the seismogram of the shot point is “divided” into time intervals based on a given number of traces. In these conditional segments, the average amplitude is determined. If the amplitude of the trace exceeds the threshold level set by the user, then it decreases to the level of average amplitude, but within the framework of user-defined coefficients. As a result of this procedure, noise is successfully attenuated, and the possibility of a differentiated approach to data at different time intervals allows this procedure to be applied, while preserving the amplitudes of the useful signal to the maximum. The parameters were interactively selected: the number of traces (= 250), and threshold coefficients for amplitudes and amplitude replacement coefficients, which varied from 1.3 to 100.

4.2.5 Suppression of the surface waves

In order to suppress low-velocity surface waves, the LFAF procedure (FK region suppression) was tested. Based on the analysis of the FK spectrum of the initial data, the following parameters were tested:

- velocity $V = 1500 \text{ m/s}; 1700 \text{ m/s}; 2000 \text{ m/s}; 2500 \text{ m/s}$
- frequency limits $0\text{-}20 \text{ Hz}; 0\text{-}25 \text{ Hz}; 0\text{-}30 \text{ Hz}; 0\text{-}35 \text{ Hz}$
- application area shot points

This procedure was tested before and after deconvolution. Based on the degree of suppression of surface waves and the preservation of the shape of the useful signal, it was decided to apply LFAF after deconvolution in the region of the shot points in the transmission mode at a velocity of $V = 2000 \text{ m/s}$ in the frequency range $0\text{-}35 \text{ Hz}$.

4.2.6 Minimum-phase conversion

Converting vibration data to a minimal phase is preferable for some processing procedures, such as deconvolution, static correction. The calculation of the operator of the minimum-phase filter is made taking into account the parameters of the sweep, discreteness, sweep frequency, sweep length. The operator converts the zero-phase signal into a minimum-phase signal.

4.2.7 Deconvolution

Single-channel deconvolution and surface-consistent deconvolution were tested.

Parameter testing performed:

- prediction interval $2, 4, 8, 12, 24 \text{ ms}$
- white noise percentage $0.1\%, 1\%, 3\%, 5\%$
- area of filter application shot points, receiver points, deletions
- number of windows one, two
- length of the operator $50 \text{ ms}, 100 \text{ ms}, 200 \text{ ms}$

In order to obtain the maximum resolution of the wave pattern and maintain traceability of the boundaries, a surface-consistent deconvolution with parameters was chosen:

- prediction interval 2 ms
- Length of operator 200 ms
- Two windows $(W100\text{-}1900), Pw1\%$ (white noise percentage)
 $(W2100\text{-}5200), Pw1\%$

4.2.8 Suppression of the noise after deconvolution

Based on the results of spectral analysis, a band-pass filter in the frequency range was selected (6,10,120,160 Hz).

In order to suppress the noise after deconvolution, the Lift technology was used.

Lift – is a method based on modeling signal and noise, and then suppressing random and coherent noise in a non-linear adaptive way.

4.2.9 Surface-matched amplitude correction

In order to compensate for the impact of complex surface-geological conditions on the amplitudes of the SP and RP, the procedure of surface-coordinated levelling of amplitudes was used. Parameter testing was performed:

window size	T100-4200 s, T100-2500 s
amplitude adjustment for shot points and receiver points	
amplitude adjustment for shot points, receiver points and deletions	

It was decided to choose a surface-matched compensation of amplitudes in a single T100-4200 window according to three factors (shot points, receiver points and deletions).

4.2.10 Refracted statics

There were no data on a priori statics. Preliminarily, the static from the relief was calculated with a datum line of **+120m** and a displacement velocity of 1700 m/s. Fluctuations in the relief and changes in surface conditions in the area affect the under-compensation of statics. It was decided to test the refracted statics.

Picking of the first entrances is carried out by the Fbnet program (Focus).

Calculation of refracted statics was carried out by the Refsol (Focus) and Renegade (SeismicStudio) programs.

It was decided to apply the refracted statics, calculated by the Refsol program with a replacement velocity of 1700 m/s and a datum line (+120m).

4.2.11 Correction of static corrections

Correction of static corrections was made after each correction of kinematics.

Parameters tested:

setting window size	200-2500 ms; 200-4100 ms
maximum shift	24 ms; 12 ms

4.2.14 Migration in the time domain

To clarify the structural image, the time migration was tested according to the initial and after summing in the time domain according to the Kirchhoff algorithm. Migration was carried out according to the hodographs of the CDP on equal removals.

Parameters tested:

percentage from smoothed velocities of summation:	90, 95, 100, 110
aperture	4.5 km, 5 km, 6 km, 6.5 km, 7 km
anti-aliasing option	triangular, in the frequency range
anti-aliasing filter	0.25, 0.5, 1
coefficient of stretch	50, 70, 100%

In the anomalous zone, time migration after summation is more preferable, than migration according to the initial effect.

The processing graph included Kirchhoff's time migration according to the initial parameters:

100% from stacking velocities (V₂), triangular method, anti-aliasing filter = 1;
aperture – 6.5 km;
coefficient of stretch 100.

Hodographs of the time migration by initials are transmitted for seismic inversion.

4.3 Testing parameters after the summation

4.3.1 Increase of signal/noise ratio

The FXY procedure identifies and applies a 3D spatial predictive filter to increase the signal/noise ratio in the frequency domain.

Parameters tested:

number of traces in the direction of the receiver line:	7, 15, 21, 41
number of traces in the direction of the explosion line:	7, 15, 21, 41
percentage of the initial trace:	30%, 50%, 60%, 70%,

Based on the degree of recording regularization and increasing the signal/noise ratio, those parameters were chosen:

the number of traces in the direction of the lines of receive and explosion:	21x21
percentage of the initial trace:	50%

4.3.2 Suppression of the regular noise. FK-filtration

FK-filtering is used to remove local regular noise without removing useful trace information.

On the cumulative cross-sections in some areas, noise, surface waves are observed.

In order to suppress them based on the analysis of the FK spectrum, we decided to apply FK-filtering (polygon) in the noise rejection mode.

4.3.3 Increase of the signal coherence

In order to suppress irregular noise and highlight the coherent component of the useful signal, the Fkpower procedure was tested.

Parameters tested:

coefficient of increase of counting of FK amplitudes - 1.1, 1.15, 1.17, 1.2, 1
Pow=1.17 coefficient selected.

4.3.4 Bandpass filtering

The bandpass filtering parameters were selected based on the analysis of frequency spectra, search of narrow-band and triangular filters.

It has been approved to apply an optimal variable by the filtering time:

T 0 – 500	(16, 2085, 105) Hz
T 1000 - 2000	(6, 10, 85, 105) Hz
T 2400 - 6000	(8, 12, 70, 90) Hz

Based on the testing results, a processing graph was generated with the application of the parameters selected on the basis of the testing described above.

4.4 Processing graph before and after summation

4.4.1 Processing graph before summation

1. Conversion from SEG-D field format into FOCUS internal format.
2. Geometry assignment.
3. Amplitude recovery: $A=A(i) \times T^N / RL^N$; $N=1.6$.
4. Pre-bandpass filter centering (4,8,160,180 Hz).
5. Suppression of noise in the zone of nearby deletions:
time-varying suppression coefficient (Gain in dB) at 35.79 removal.

6. Suppression of amplitude anomalies (noise traces, sound wave) in the area of the shot points: median filtering Ampscale. Lift- technology.
7. Shot point amplitude correction (T0-6000s.).
8. Minimum-phase transformation.
9. Refracted statics.
10. Surface-matched deconvolution with parameters:
 - operator length 200 ms
 - prediction interval 2 ms
 - 2 application windows 1 (W100-1900), Pw 1% (percentage of the white noise)

2(W2100-5200), Pw 1%
11. Bandpass filter: (6,10,105,125) Hz.
12. Surface wave suppression. Low-velocity spatial filtering LFAF (velocity V=2000m/s in the frequency band 0-35 Hz).
13. Editing of traces. Irregular noise suppression (Lift technology).
14. Surface-matched amplitude correction:
 - adjustment of the amplitudes for shot points, receiver points and deletions in the window
 - T100-4200ms.
15. First correction of kinematic corrections.
16. First correction of static corrections.
 - setup window 200 – 4100 ms
 - maximum shift 24 ms
17. Second velocity correction, analysis step (X=500m, Y=250m)
18. Second correction of static corrections
19. Increase of coherence in the FK domain.
20. Residual statics.
21. Time migration by input (Kirchhoff's algorithm):
 - aperture 6.5km, triangular method, 100% of smoothed velocities of summation.
22. Velocity analysis (3rd iteration)
23. Summing with final muting.

4.4.2 Processing graph after summation

1. Application of FXY-filter (percentage of adding the initial trace 50%)
2. Suppression of regular noise (FK filter in rejection mode).
3. Increase of the coherence of a useful signal. Fkpower=1.17.
4. Bandpass filtering variable by time
 - T 0 – 500 (16, 20 85, 105) Hz
 - T 1000 – 2000 (6,10,85,105) Hz

- T 2400 – 6000 (8,12,70,90) Hz
5. Scaling

4.5 Depth migration before summation (PreSDM)

Depth migration according to the initial data before summation (PSDM) was carried out on the Saigak contract area. Processing was performed by «SGS» LLP using POWER 2D/3D GeoDepth (Paradigm Geophysical) processing packages and Epos2011.3 (Echos) software package developed by Paradigm company. The work was carried out from the datum line +120 m.

4.5.1 Goals and objectives of the deep migration before summation

Work on the deep migration according to the initial data before summation within the Saigak deposit - 32 km² with a bin of 12,5 ×12,5 m.

The main goal of deep migration – is to reliably trace the horizons of the Permian-Triassic complexes, to identify faults, including low-amplitude ones, to more accurately beat out the surface of the salt and subsalt horizons, as well as to obtain a deep-velocity model that allows you to obtain reflecting boundaries at a deep scale. All of this allows us to identify in detail the structural features of the area associated with the presence of hydrocarbon traps.

4.5.2 Initial data loading

As the initial data, we used the results of time processing with the input of all parameters that increase the signal/noise ratio and recording resolution: edition, amplitude adjustments, filtering, and muting.

a) initial seismograms sorted by CDP with a priori and corrective corrections introduced

b) cumulative time volume

c) time migration cube after summation

d) cube of summing velocities

After loading, a checksum was obtained to verify the input data.

4.5.3 Construction of a velocity model

To build a depth-velocity model, the calculation of the spectra of interval and reservoir velocities is performed on the inline and crossline network. The distance

between the lines was chosen evenly over the entire area and was 250 m by inline and crossline (12,5 m. * 20 inl./cr. = 250 m.).

At the first stage of constructing a depth-velocity model, it is necessary to choose dynamically expressed conditional horizons that describe the time cross-section in sufficient detail. For this project, 8 supporting horizons were selected, which are correlated over the entire area and linked at the intersection points, outlined for the construction of the model. An example of correlation of conditional horizons in the time domain is illustrated in Figures 4.1 - 4.2. At the stage of correlation and analysis of the wave field of the deposit, attention was paid to the features of the wave pattern in the central part of the area. On cross-sections passing through this area, we are able to manifest complications of the nature of seismic recordings associated with a decrease in the multiplicity. The multiplicity map is illustrated in Figure 3.1.

Interval velocities for each horizon were calculated by the method of coherent inversion, implemented in the «GeoDepth» program. For each t_0 of the tracked boundary, is determined the coherence of the axes of phase synchronism for each enumeration of the interval velocity, which shows the degree of straightening of the hodograph for a given velocity. The range and enumeration step of the velocities is determined in the local testing mode. For the first 30 horizons, the step is 25 m / s, for the rest - 50 m / s.

Velocity Vint, which straightens the hodograph in the best way, will give maximum coherence in the horizontal spectrum. The resulting graphs are tracked and linked together at the intersections of the profiles. The graph represents the value of interval velocity for a given formation. Figures 4.3 - 4.6 illustrate examples of the coherence spectra of interval velocities and their interpretation.

After linking the spectra of interval velocities along the first horizon using radiation migration, we recalculate the first horizon from the time domain to the depth along the 3D profile grid and build the velocity model to the first horizon. With this model, we calculate intermediate depth migration for each 20 inline and crossline, specifying the picking in depth, linking it at the intersections. In this case, we obtain maps of the first supporting horizon in depth and the corresponding map of the interval velocity till the first horizon.

After that, we move to the next horizon, layer-by-layer increasing the velocity model from the overlying to the underlying horizon along the entire depth of the cross-section with the account of intermediate migrations to the last horizon, getting the final velocity model, see figures 4.7 - 4.8. Figure 4.9 illustrates a map of depths and a map of interval velocities up till 4th supporting horizon.

After each intermediate migration through deep selections, we perform residual kinematic analysis. For this, we calculate the vertical spectra of residual kinematic corrections, which allow us to control the degree of straightening of the hodographs

of the reflecting boundaries, and, consequently, the degree of accuracy of the interval velocity to each boundary.

4.5.4 Testing parameters of depth migration (PreSDM)

One of the main parameters affecting the quality of deep migration is the aperture. In the migration procedure of the Paradigm company, the aperture is defined as the maximum displacement of the seismic data that must be fully displayed by the migration. When choosing an aperture, two factors are taken into account: the maximum angle of inclination of the boundaries and the maximum depth.

In this area, deposits of interest from the point of view of prospectivity for the presence of hydrocarbons occur from 1.6 km and below. There are no large tilt angles on the area. Additionally, for the final migration an anti-aliasing filter was tested. Using an anti-aliasing filter allows to reduce high-frequency noise.

Thus, the following parameters were selected for the final depth migration from the initial data before summation:

- Depth – 12 000 m, discretization step 4 m
- Aperture for Kirchhoff Migration - 7000 m
- Kinematic Muting (stretch)- 100%
- Anti-aliasing filter (optimum noise level reduction)- 1 (median strength).

4.5.5 Residual analysis and post-migration processing

A residual kinematic analysis of the results of the final migration is used to improve the summation. It allows us to take into account the high-frequency component of errors of the high-speed model. The calculation of the vertical spectra for the selection of the residual kinematic correction was carried out with a step of 250 m, then a total depth cross - section was obtained with the mute selected by the depth selections and the input of the residual kinematic corrections. Then, the deep cross - sections were recounted in the time domain to perform time processing procedures in the Epos2011.3 (Echos) system, which are aimed at suppressing multiple waves and improving the coherence of the wave field. After performing these time processing procedures, data is recalculated from the time - back to the deep region.

4.5.6 Wells

The customer transmitted the data on wells located in Saigak region. Basically, there are 8 wells, which are situated directly in the area, the data for which

were used for analysis. Wells have the appearance of highly variable inclinometry. An example of location of the wells is illustrated on the map and seismic cross - section. See figures 4.10 - 4.11.

After analysis and evaluation of the binding of the wave field to the borehole data, the data was transmitted for the further interpretation process. The result of the binding of the Saigak-6 well is illustrated in Figures 4.12 - 4.13.

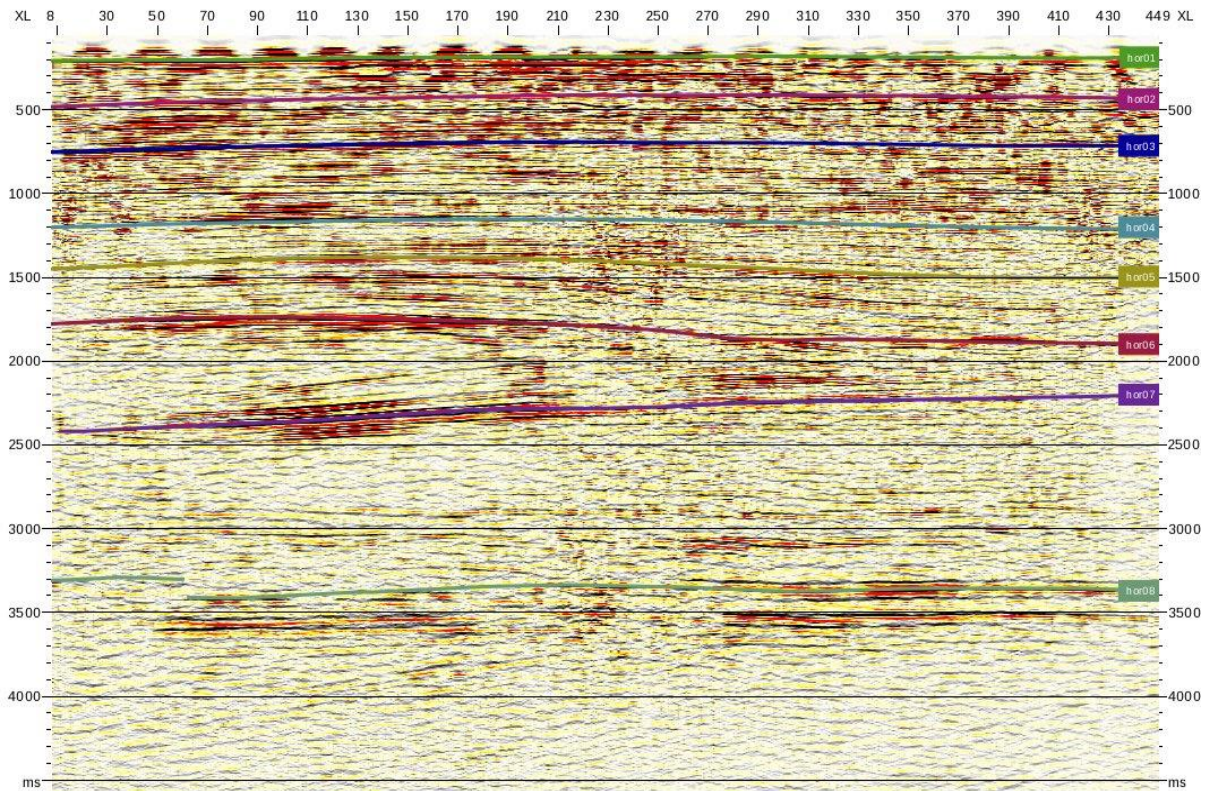


Figure 4.1 – Time cross-section, inline 181 with 8 supporting horizons for V int calculation

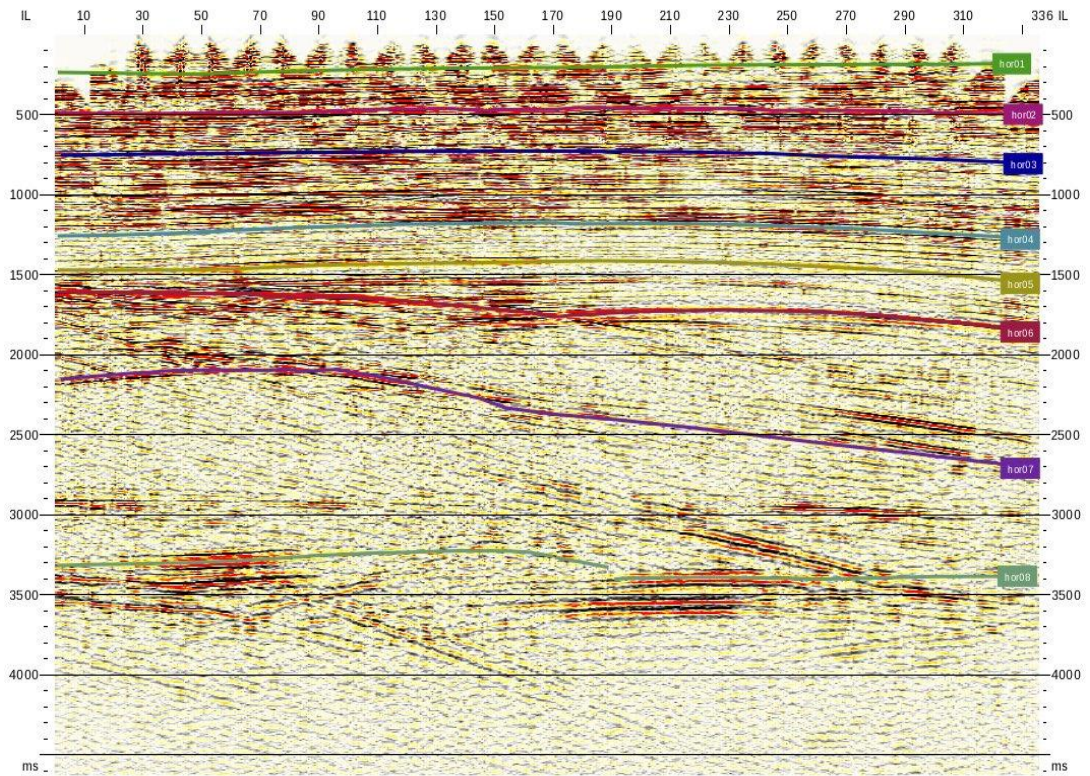


Figure 4.2 – Time cross-section, crossline 60 with 8 supporting horizons for V int calculation

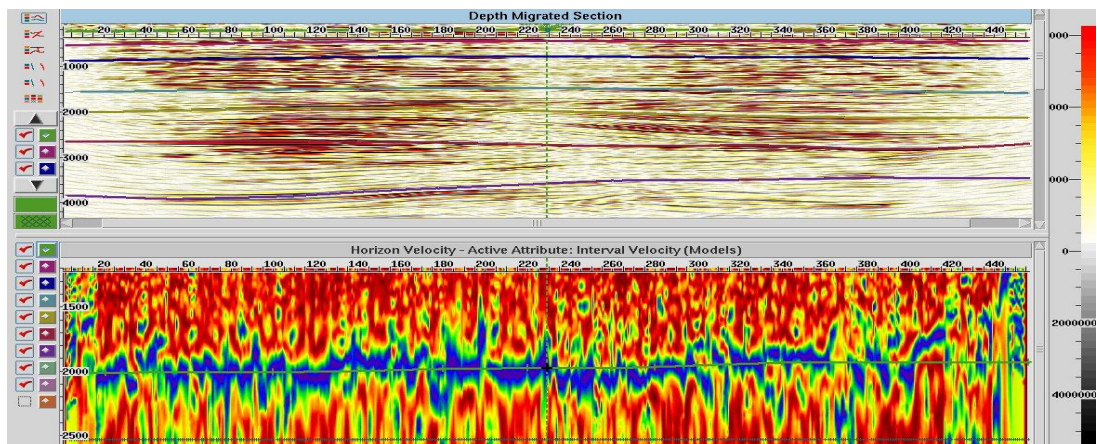


Figure 4.3 – Spectrum of interval velocity up to the 1st horizon (inline 141)

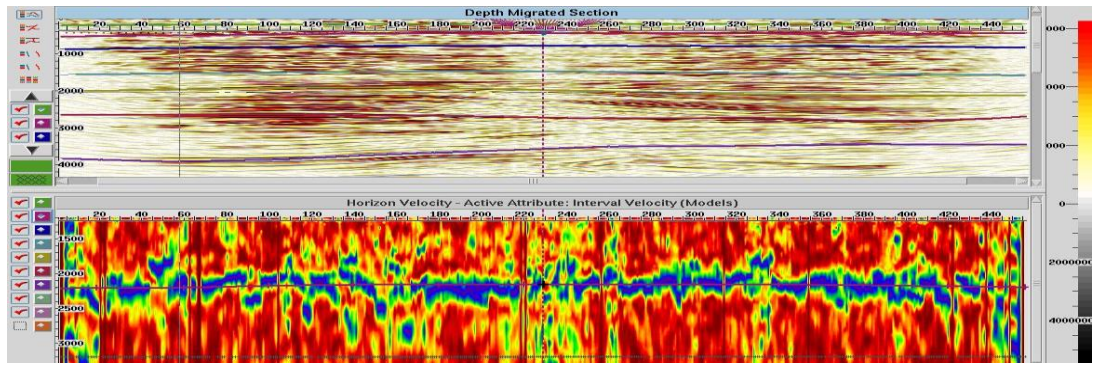


Figure 4.4 – Spectrum of interval velocity up to the 2nd horizon (inline 141)

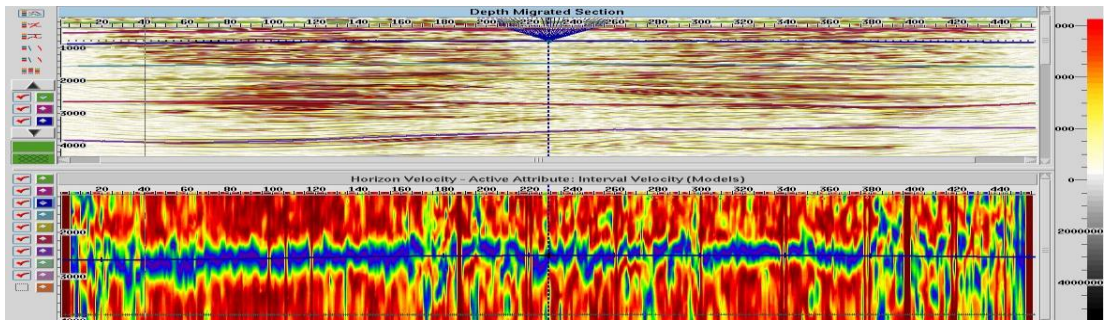


Figure 4.5 – Spectrum of interval velocity up to the 3rd horizon (inline 141)

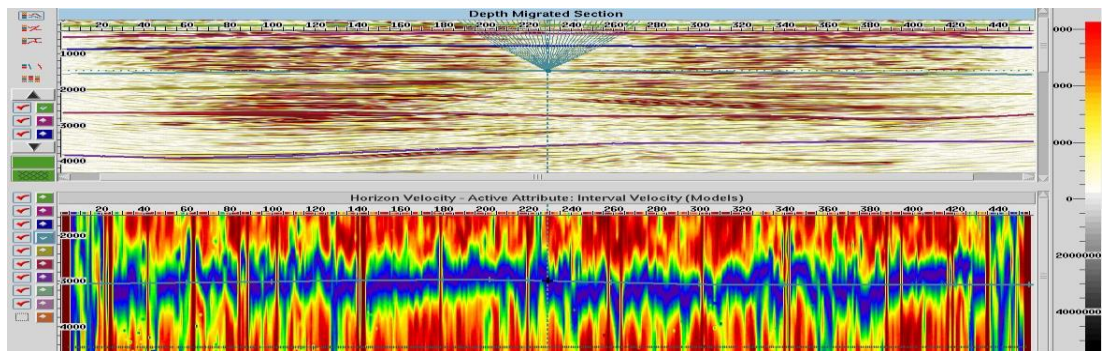


Figure 4.6 – Spectrum of interval velocity up to the 4th horizon (inline 141)

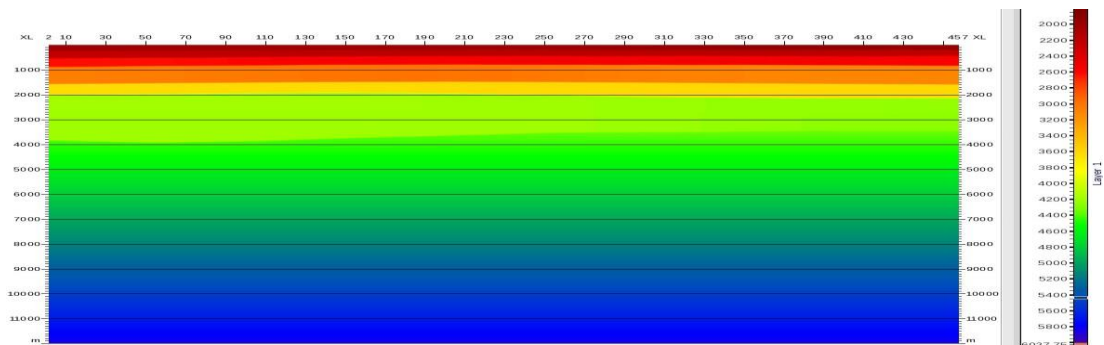


Figure 4.7 – Final section of interval velocity (inline 141)

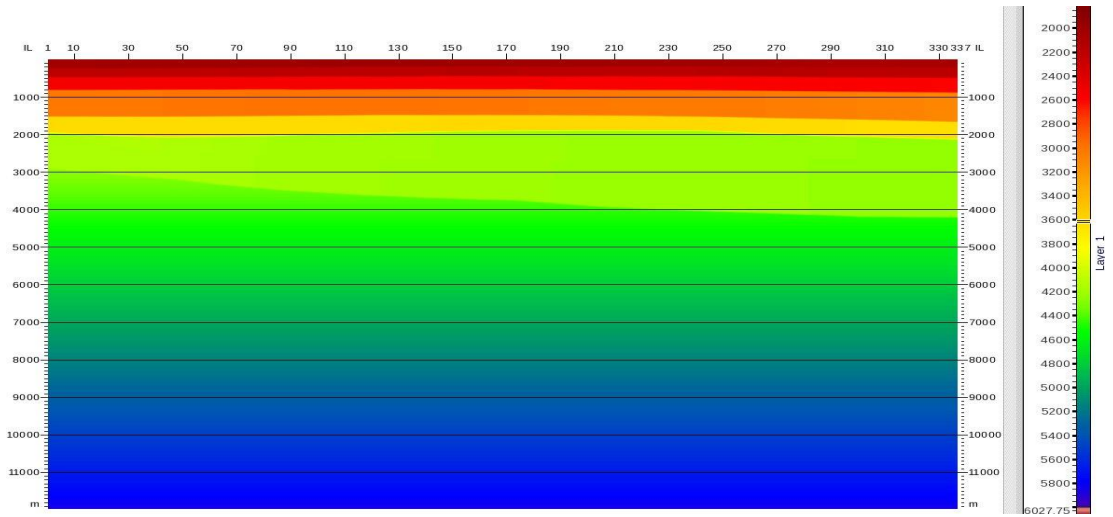


Figure 4.8 – Final section of interval velocity (crossline 180)

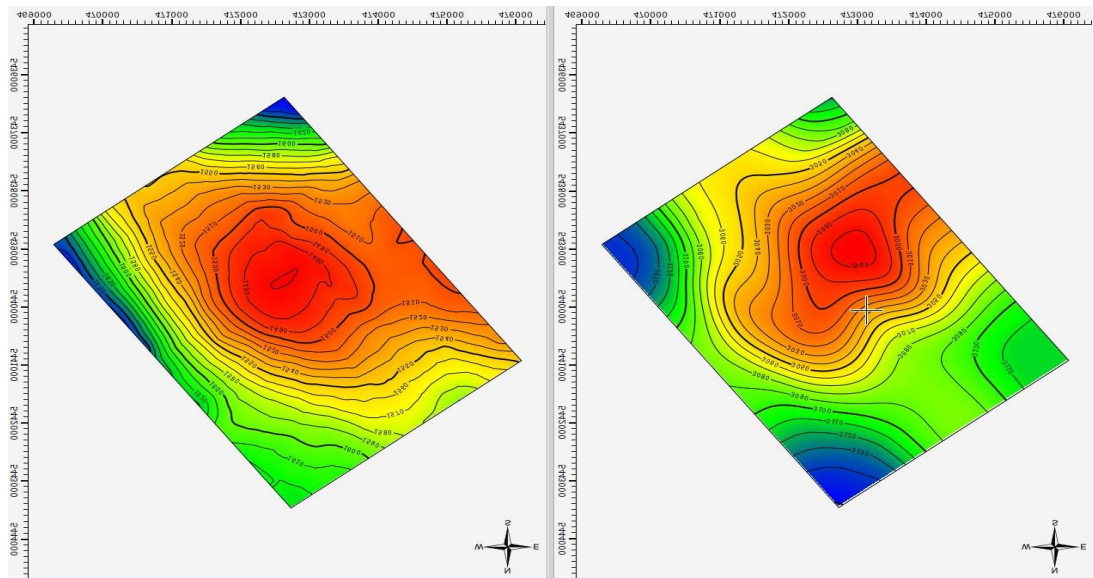


Figure 4.9 – Map of depths and interval velocities up to the fourth supporting horizon

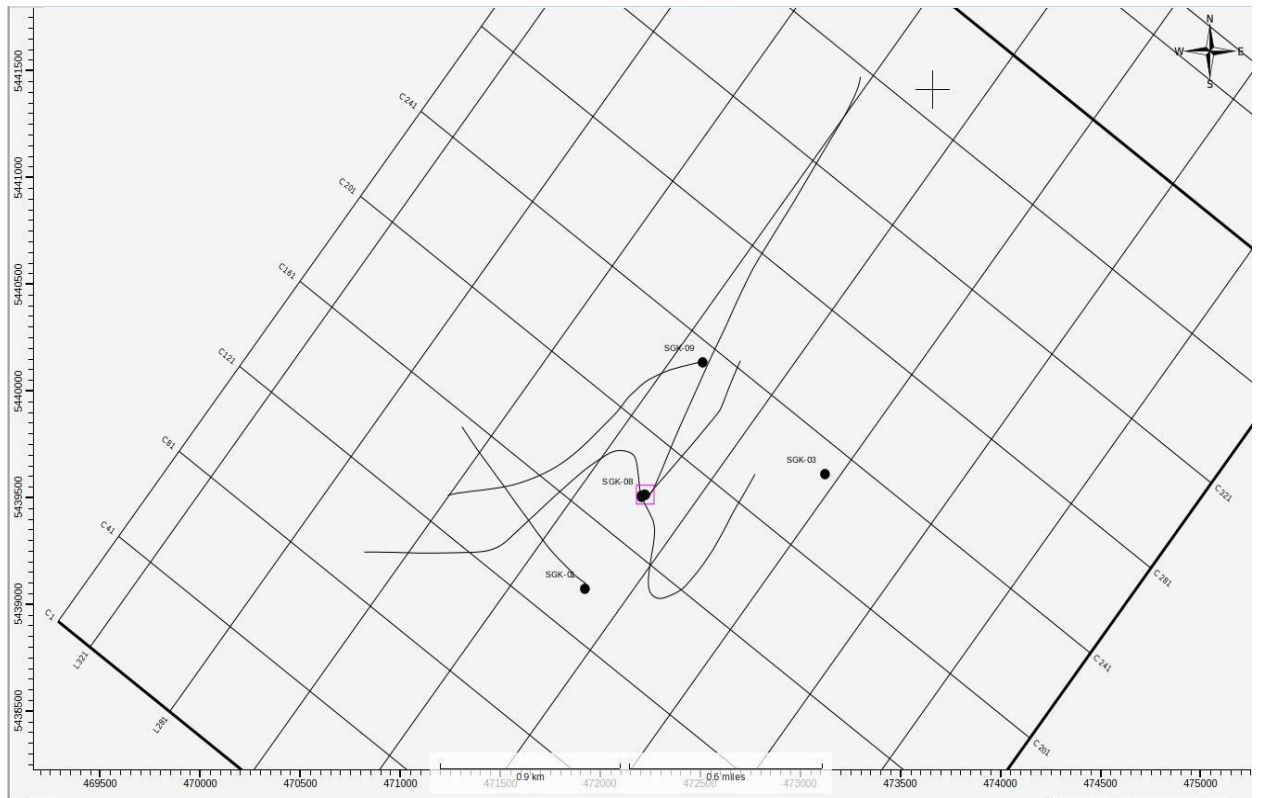


Figure 4.10 – Well location map

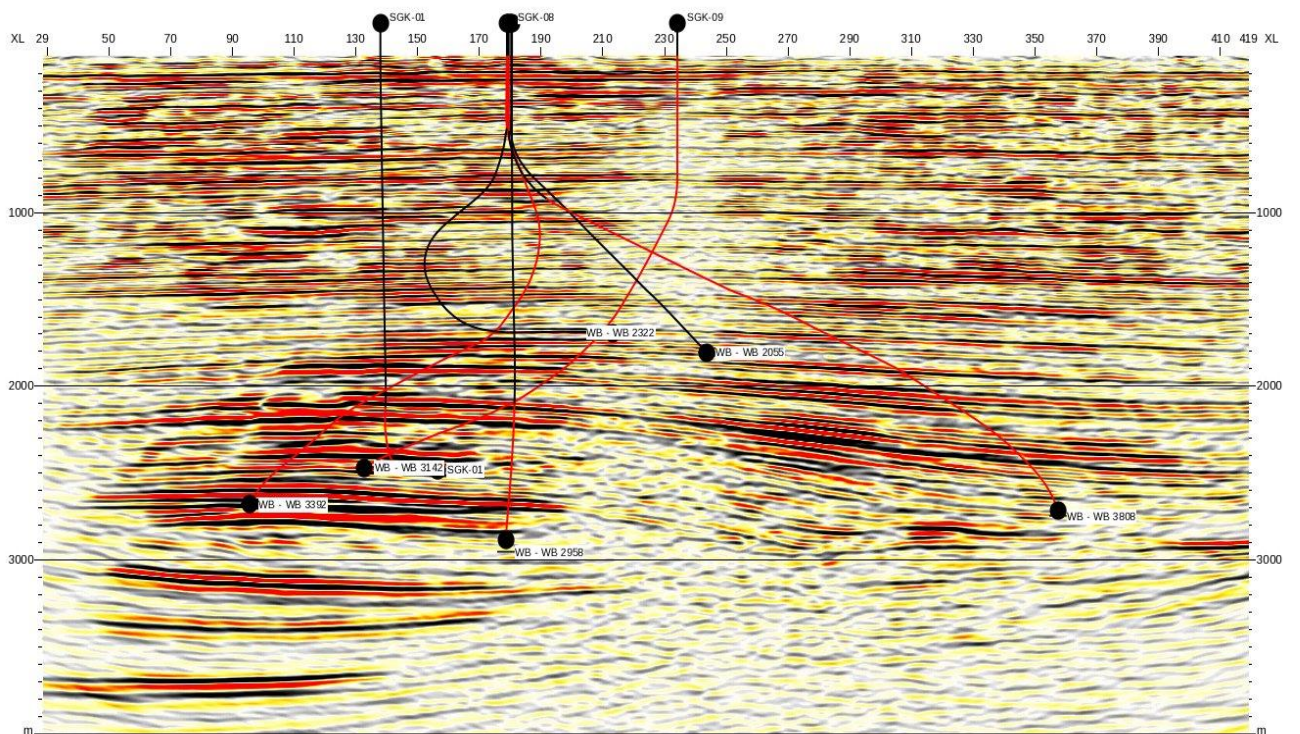


Figure 4.11 – Location of wells on seismic map

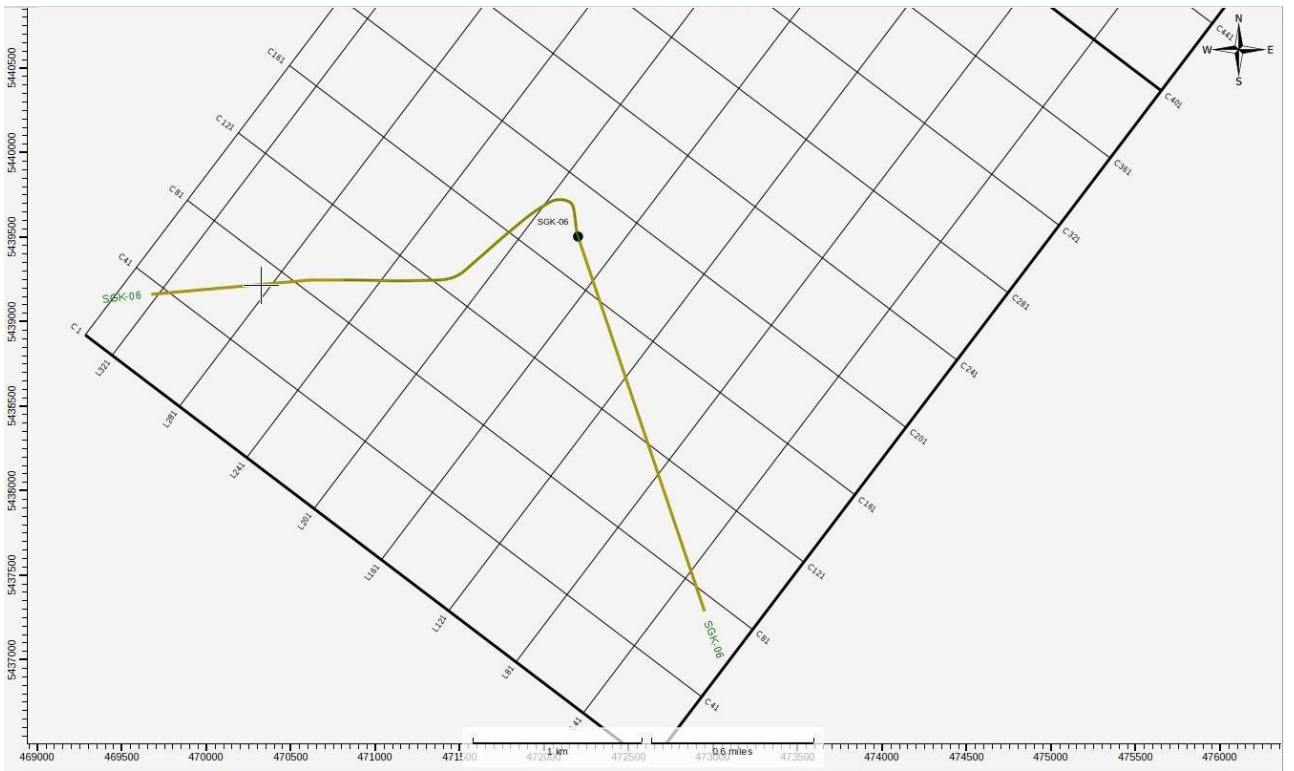


Figure 4.12 – Traverse through the SGK-06 well on the map

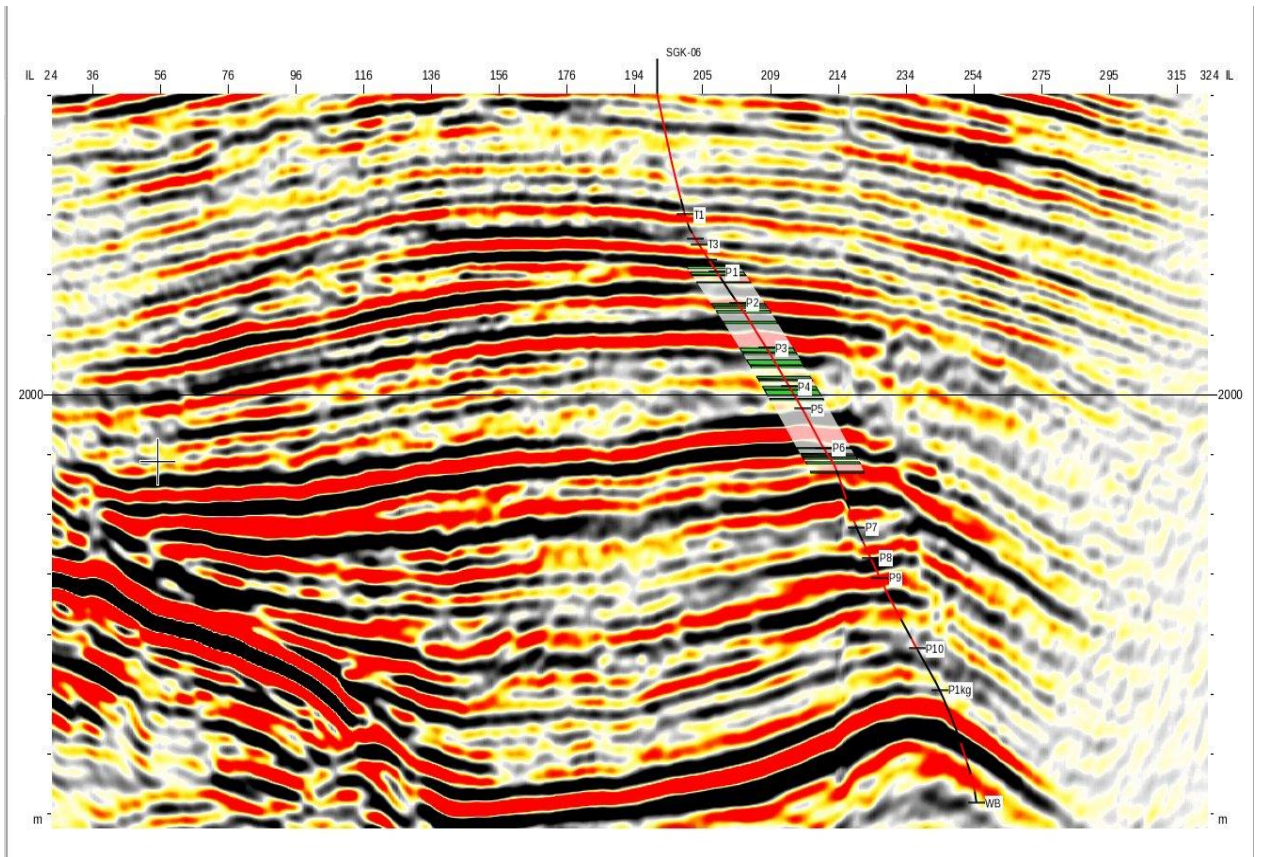


Figure 4.13 – Traverse through a well on seismic

4.6 Conclusion of the Processing part

Analysis of the resultant materials illustrates that the procedures aimed at suppressing the noise (Ampscale, Lift-technology), increasing resolution (deconvolution), traceability (refracted statics, static correction), increasing the coherence of the useful signal, the structural image clarification (migration by source) were applied effectively for the processed area.

The selected and applied parameters, the data processing graph made it possible to solve, mainly, the geological problems of the structural study of reflecting horizons in the Upper Permian and Triassic complex.

As a result of the reprocessing of 3D seismic data for this area, good quality deep cross-sections with a dynamically expressed wave pattern and with fairly reliable traceability of the reflected horizons were obtained.

Conducting PreSDM according to the initial data allowed us to see the structural specifics of the structure in the deep region, clarifying the presence or absence of faults. Basically, PreSDM 3D depth migration gives the interpreter the ability to link closer to reality correlation of target horizons in the geological zone of interest. Deep migration made it possible to link well markers and traced horizons in deep cross-sections, providing the customer with information on the depth migration velocities as well.

5 Interpretation of geological and geophysical materials

The interpretation of geological and geophysical materials consisted of two stages: structural and dynamic. The interpretation was carried out using the software of the Paradigm company.

5.1 Structural interpretation

Structural interpretation is the basis for compiling a model of the geological structure of the working site. At this stage, the following types of work were performed:

- the formation of the project in the work station;
- alignment of the wave field with the well-logging data and stratigraphic splits;
- correlation of the target reflecting horizons in time cross-sections;
- correlation of the target reflecting horizons in depth cross-sections;
- construction of structural maps;
- construction of thickness maps between supporting RH.

5.1.1 Stratification of reflecting horizons

Within the considered area, well-logging materials were used in the process of stratification of supporting reflecting horizons.

In full accordance with the tasks to be solved, seismogeological zoning and allocation of seismogeological floors were used. During the interpretation, the indexation of supporting horizons for the suprasalt rock complex was agreed with the customer.

- T-1 – lower triassic;
- T-2 – lower triassic;
- PT– permo-triassic;
- P-1–tatarian stage of the upper permian P_{2t} ;
- P-2– tatarian stage of the upper permian P_{2t} ;
- P-3– tatarian stage of the upper permian P_{2t} ;
- P-4– tatarian stage of the upper permian P_{2t} ;
- P-5– tatarian stage of the upper permian P_{2t} ;
- P-6– tatarian stage of the upper permian P_{2t} ;
- P-7– tatarian stage of the upper permian P_{2t} ;
- P-8– tatarian stage of the upper permian P_{2t} ;
- P-9– tatarian stage of the upper permian P_{2t} ;
- P-10– tatarian stage of the upper permian P_{2t} ;
- P_{1kg} –roof of kungurian stage of the lower permian.

Structural constructions were completed for all marked horizons, on the basis of which the structure of the suprasalt complex of lower triassic and upper permian rocks was studied.

5.2 Data interpretation of the wells

Before the beginning of the works on reinterpretation of wells, all materials were analyzed, taking into account well testing, with core analysis data (figure 5.2). Graphs of acoustic and density logging are normalized in clay intervals.

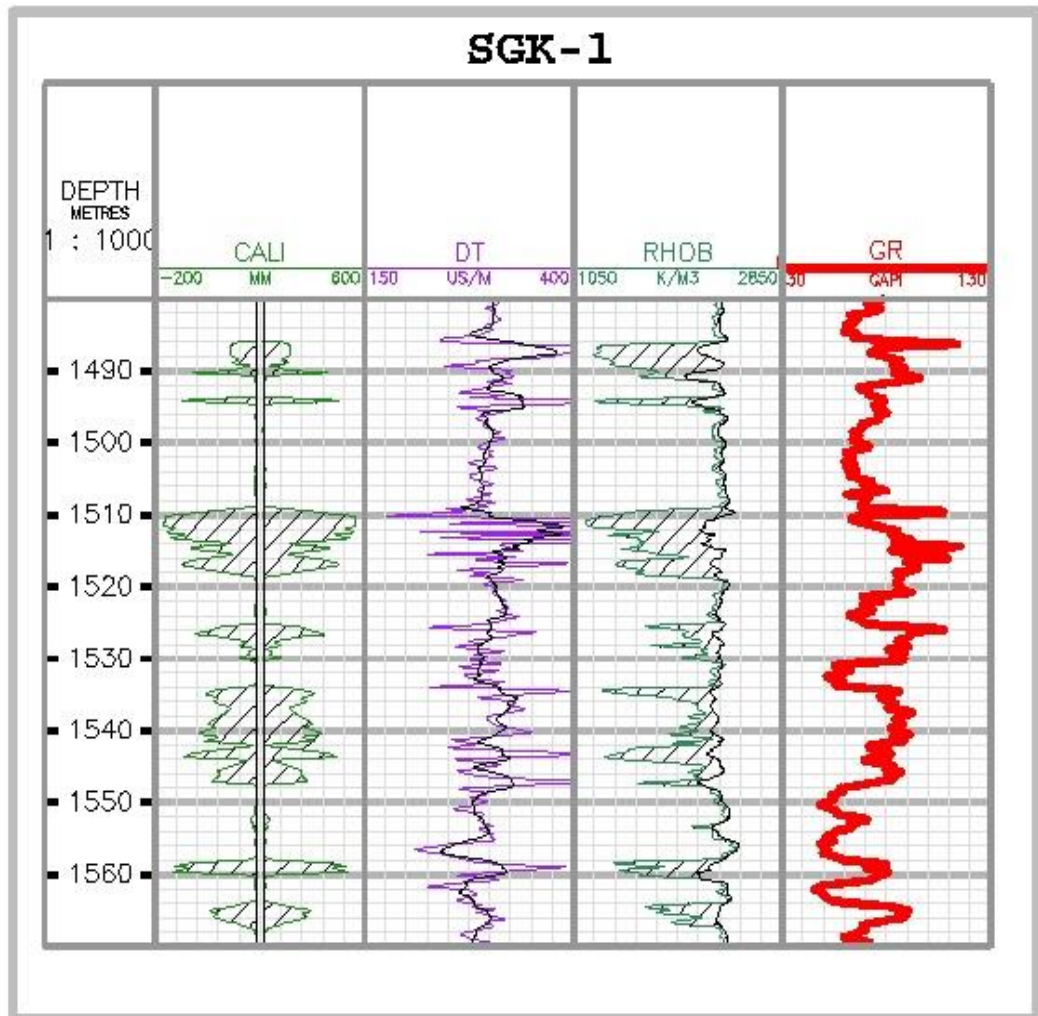


Figure 5.1 – Correction of AL and GGL-D data

The restoration of acoustic and density logging in the intervals of cavities was carried out according to empirical dependencies:

- Faust equation

$$DT = 513,3/(DEPTH*RT)*(1/6)$$

- Lindseth equation

$$RHOB = (VP-3460.)/(0,308*VP)$$

- Gardner equation (Gardner-Gardner-Gregory):

$$RHOB = a*VP^{0,25+c}$$

5.2.1 Clay content calculation

The clay content of the reservoirs was determined by the GL method, and in order to exclude the influence of the measurement conditions in the wells and the individual characteristics of the gamma-logging equipment, a double difference GL parameter was used.

$$\Delta I\gamma = (I\gamma_{nl} - I\gamma_{min}) / (I\gamma_{max} - I\gamma_{min})$$

where $I\gamma_{nl}$, $I\gamma_{max}$, $I\gamma_{min}$ - the intensity of gamma radiation against the interpreted layer and both maximum and minimum in the cross-section.

The estimation of the bulk clay content K_{cl} was determined by the equation of V.V. Larionov:

$$K_{cl} = 0,33*(2^{2*\Delta I\gamma} - 1)$$

5.2.2 The calculation of the coefficient of porosity

The determination of porosity was carried out by a set of methods for porosity loggings: acoustic, density and neutron (figure 5.2).

Porosity by AL was calculated using the average time equation with a correction for clay content:

$$Kn_{AK} = (\Delta T - \Delta T_{CK}) / (\Delta T_{\mathcal{K}} - \Delta T_{CK}) - K_{2L}(\Delta T_{2L} - \Delta T_{CK}) / (\Delta T_{\mathcal{K}} - \Delta T_{CK})$$

where:

ΔT_{CK} - travel time in the skeleton of the rock, taken equal to 175 μ s/m;

$\Delta T_{\mathcal{K}}$ - travel time in a liquid, taken equal to 620 μ s/m;

$\Delta T_{\mathcal{K}}$ - the travel time in clays was determined by the nearest strata of blurred clay.

The determination of porosity by density logging was carried out according to this equation:

$$Kn = (\sigma_{CK} - \sigma_n) / (\sigma_{CK} - \sigma_{\mathcal{K}})$$

where σ_{CK} - rock skeleton density, $\sigma_{sk}=2.68$ g/cm³, was determined as the average value of the density of grains according to core analyzes, the density of reservoir fluids σ_l was taken as 1.1 g/cm³.

According to neutron logging, in the process of porosity determination this expression was used:

$$Kp = W - Kcl \times Wcl$$

where W – hydrogen content (neutron porosity),
Wcl – hydrogen content of clay is taken equal to 0.30.

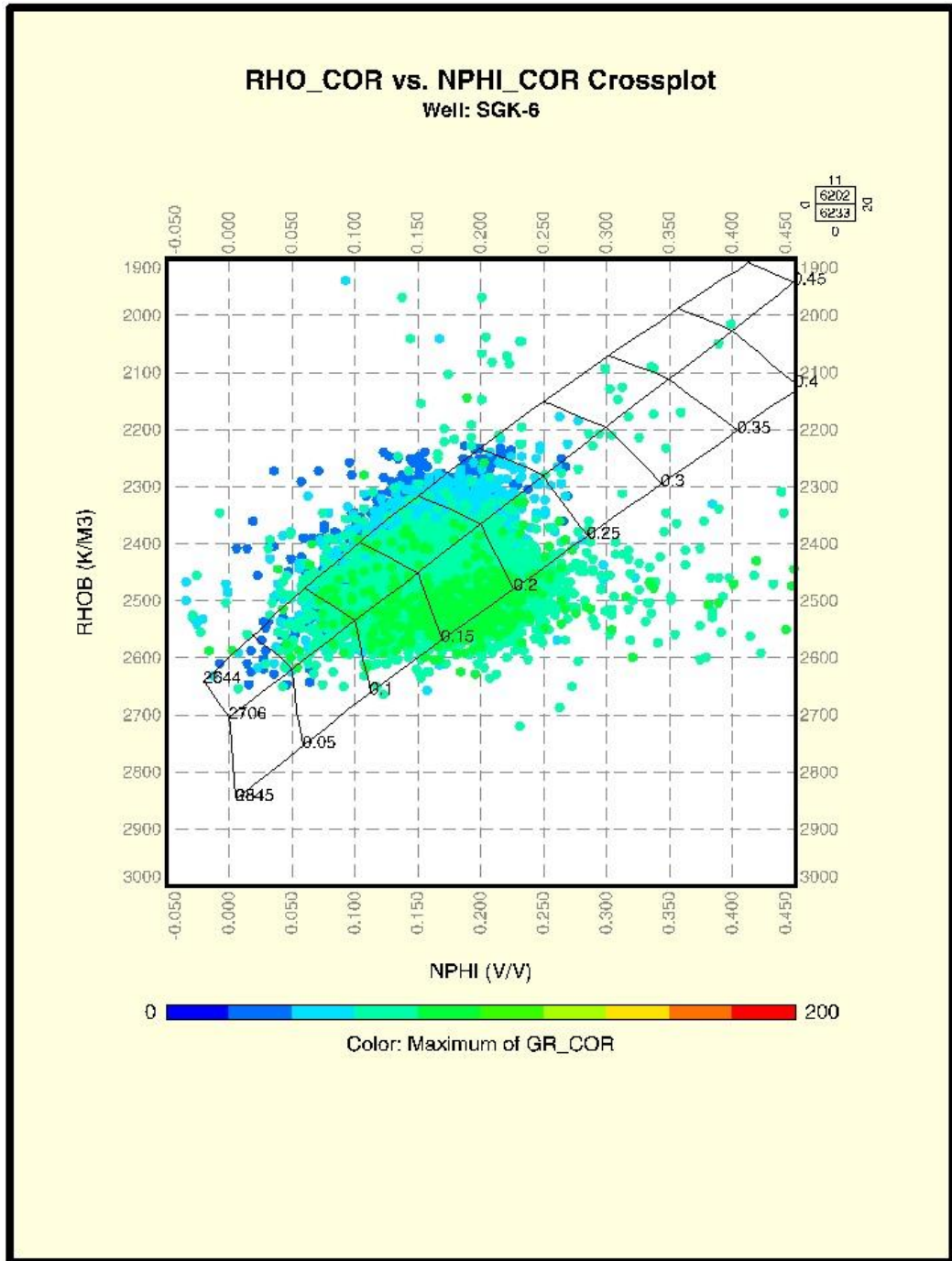


Figure 5.2 – Crossplot RHOB-NPHI-GR for calculating total porosity

5.2.3 Saturation calculation

Calculation of water saturation was carried out according to the Archie equation, the following parameters were used as input parameters:

$$S_w = (R_w / (R_t * PHIE^m))^{1/n}$$

R_t - electrical resistivity of the formation zone, not affected by the penetration, was estimated by electric logging of the far zone;

R_w - the electrical resistivity of formation water, taken equal to 0.027 Ohm;

$PHIE$ - open porosity;

a - the tortuosity coefficient is taken equal to 1;

m - the indicating degree of cementation is taken to be 1.84 by the petrophysical dependence of the porosity parameter on porosity obtained from the core studies from Saigak-1 and 2 wells;

n - saturation index, taken equal to 2 by measuring the coefficient of growth in resistance on core samples from well 2.

In addition, Pickett plots were used, which are used to determine the water resistance R_w and saturation constants. The R_o isoline is determined by the condition

$$S_w = 100\%.$$

Example of a complex interpretation of well-logging for the Saigak-2, Saigak-1 and Saigak-6 wells is illustrated in figures 5.3 - 5.4.

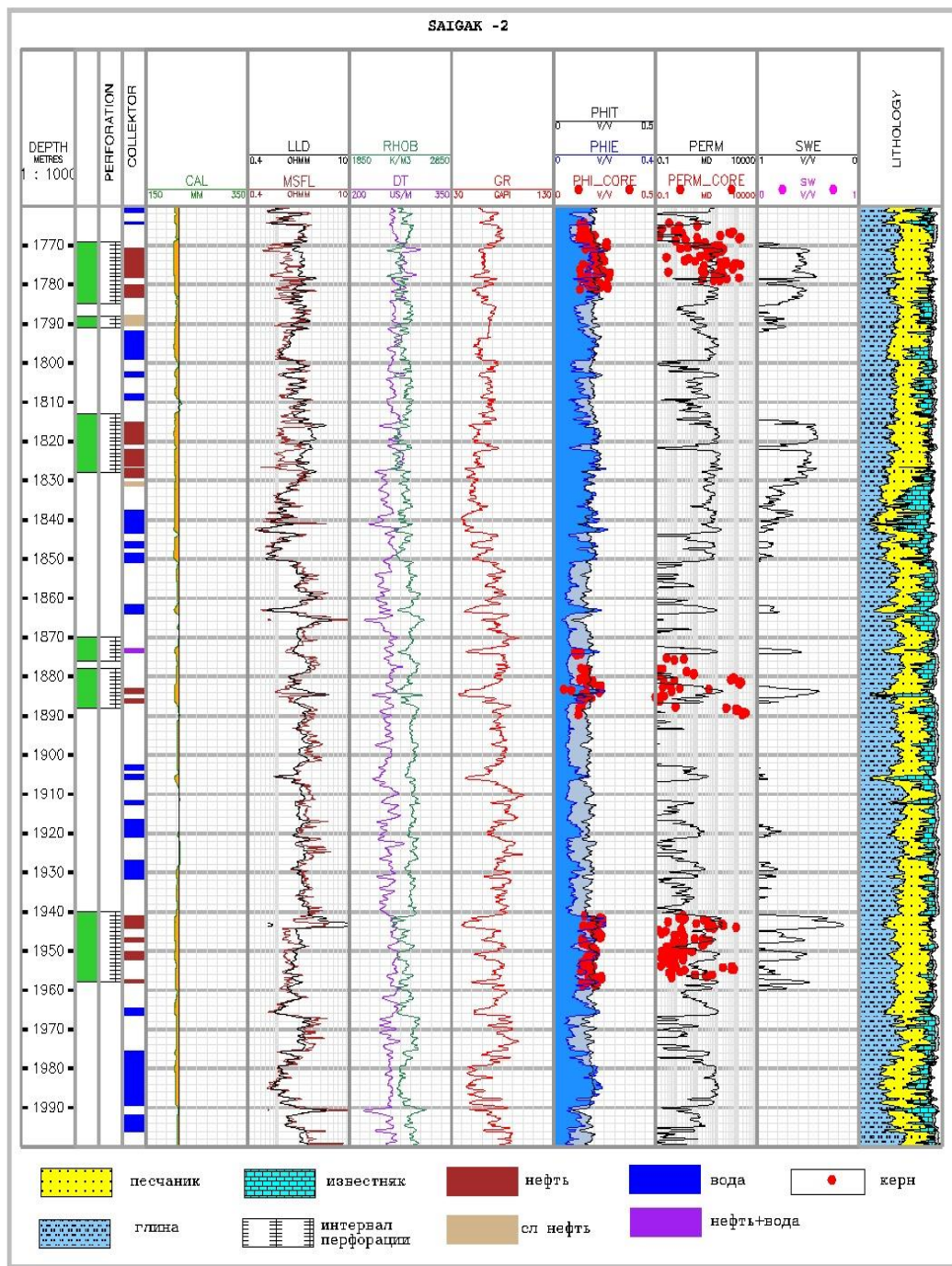


Figure 5.3 – An example of a complex interpretation of well-logging in the Saigak-2 well, as well as a comparison of porosity and permeability according to well-logging data and core data

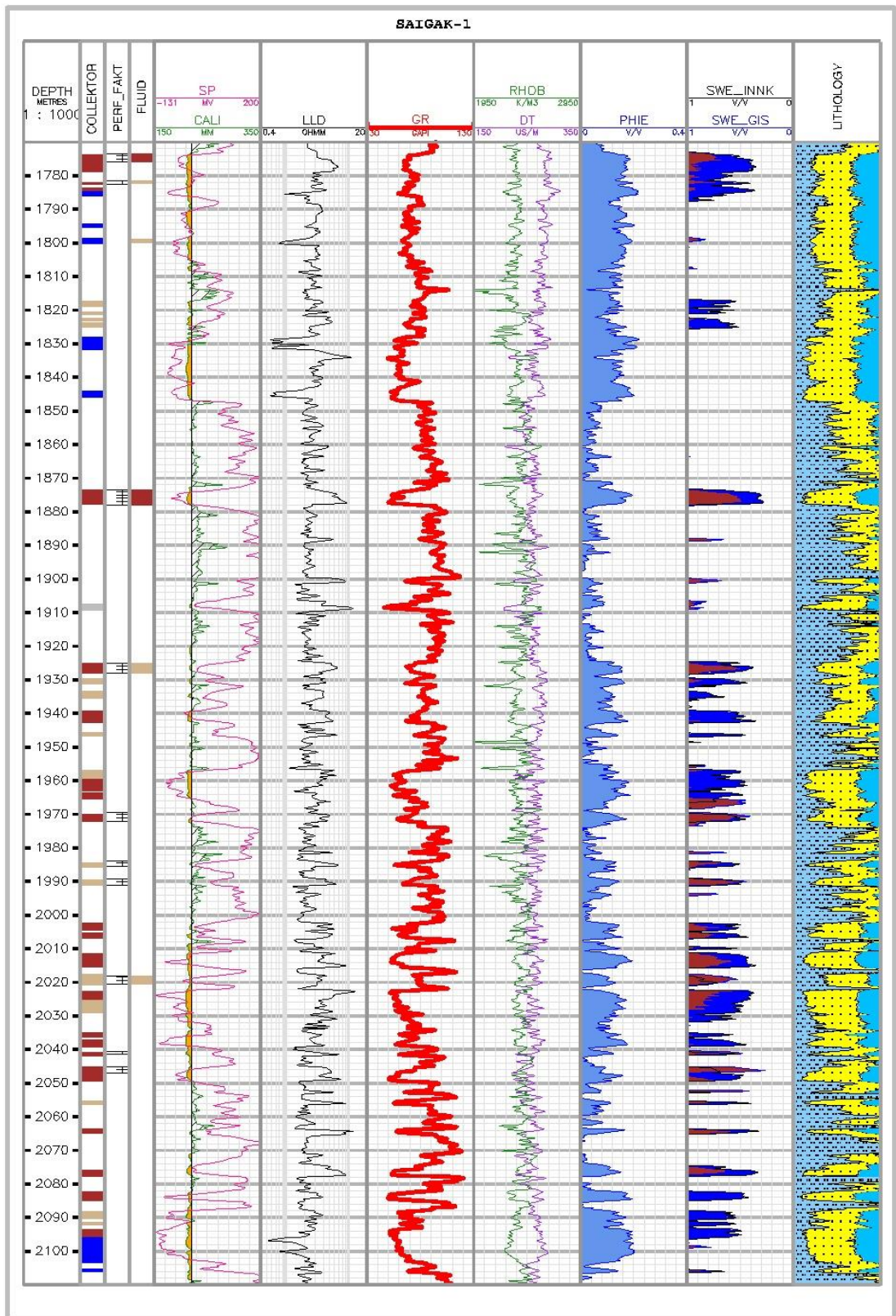


Figure 5.4 – An example of a complex interpretation of well-logging in the Saigak-1 well, as well as INNL data to determine the current saturation

5.2.4 Acoustic impedance

In order to establish a relationship between the capacitive properties, determined at the points of the wells, and the elastic characteristics of the medium that affect the propagation of seismic waves, the acoustic impedance (P_IMPEDANCE) was chosen, which is defined as the product of the density of the rock and the velocity of the longitudinal wave over the rock. P_IMPEDANCE, firstly, characterizes the rock hardness and, consequently, correlates well with lithology, porosity, saturation, and etc. And secondly, it is closely related to the dynamic characteristics of the reflected waves.

Acoustic logging acts as a direct method for estimating reservoir velocities, and gamma-gamma logging for bulk density. In order to solve this problem, it was necessary to calculate the porosity coefficient in the well.

A linear relationship has been established between the values of acoustic impedance calculated from the well-logging data and porosity coefficient in the studied interval. With increasing porosity of the rocks, the values of P_IMPEDANCE in the studied interval decreases. Such dependence may indicate, with high probability, that knowing the impedance values, it is possible to predict the porosity of the reservoir of permeable complexes.

5.2.5 Lithofacial analysis

According to the well-logging data, lithofacial analysis was carried out in 27 classes. In the calculation of lithofacies, logging curves were used that most accurately classify reservoirs by porosity, clay content and saturation. According to the GL data was calculated clay content (VSH), density logging (GGL-D), neutron porosity (NPHI) and lateral logging (reservoir resistance). Each class of facies has a certain colour scale that is related to a certain set of physical characteristics associated with claying or compaction.

Furthermore facies, similar in lithotype, were combined into 4 classes, each class was assigned a lithological characteristic representing a cross-section of wells - clays, sandstones and siltstones.

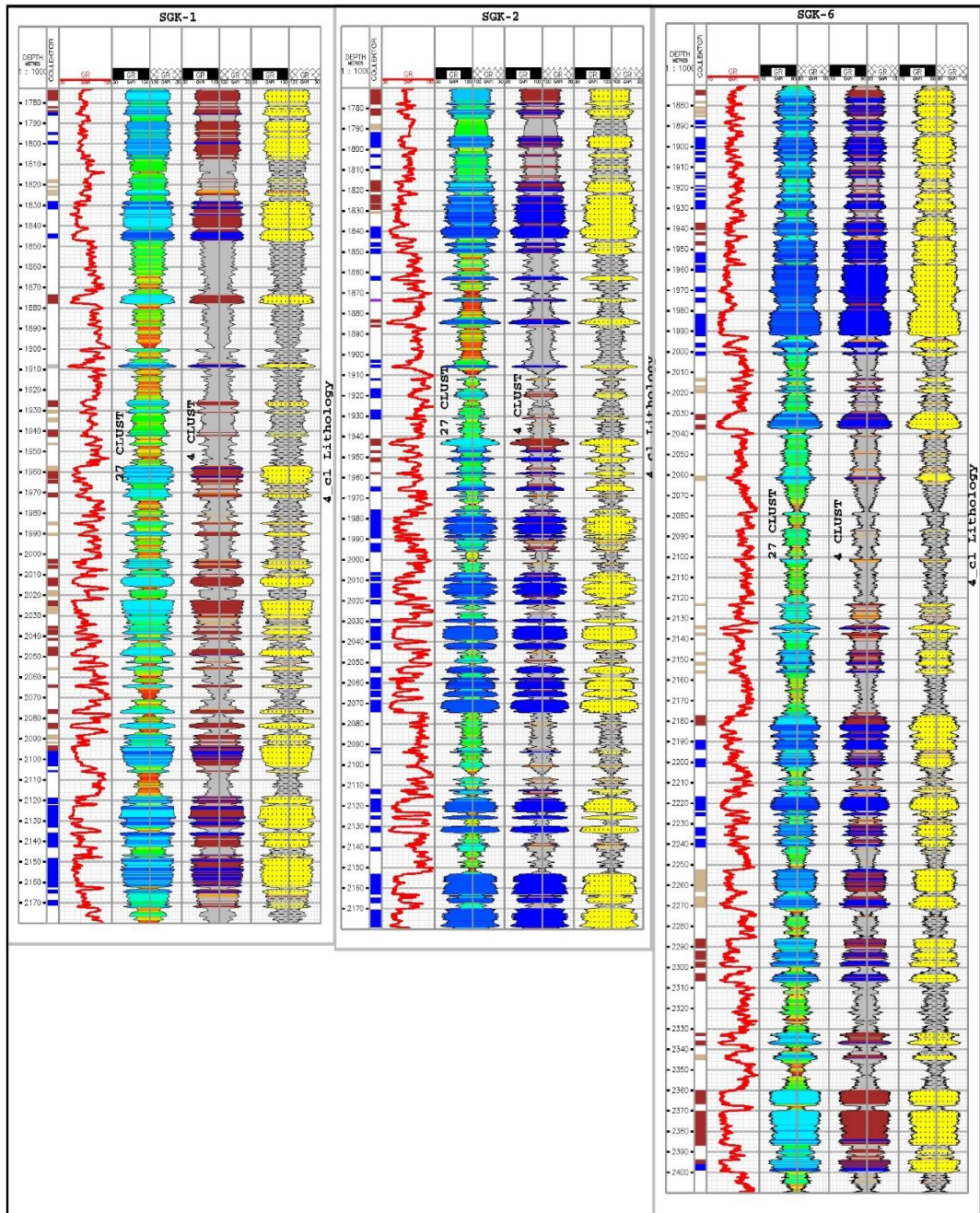


Figure 5.5 – Example of lithofacial analysis for wells SGK-1, SGK-2 and SGK-6

5.3 Seismic inversion

The seismic wave field inversion method is a mathematical seismic modeling method that integrates a dynamic interpretation of seismic data with drilling results, as well as detailed studies using the well-logging methods. To the current date, this method is happening to be the most effective tool for solving problems of predicting a geological cross-section.

To construct an acoustic model of the medium, a synchronous complete inversion of the migrated seismograms of the summation was performed on the basis of the maximum likelihood algorithm (PMLI - inversion). Main features and benefits of this inversion:

- inventors each trace of CDP seismograms;
- uses migrated offset and corner seismograms of any type at the input, as well as any angular sums.

Preprocessing of seismograms is performed during the inversion process, taking into account the effect of signal stretching along the offset for each trace.

Allows to obtain elastic properties: P-impedance, S-impedance, Vp and Vs, Vp / Vs, Poisson's coefficient, LR, MR and synthetic seismograms.

8 wells have been drilled in the Saigak area, SGK-01, SGK-02, SGK-03, SGK-04, SGK-06, SGK-07, SGK-08, SGK-09. In the wells SGK-01 and SGK-03, there is no transverse wave data (DTS) of acoustic logging, so for these wells transverse wave velocity was calculated by the formula: $DTS = (-52.5846 + 2.06275 * DT)$. The data of density, longitudinal and transverse waves were further used to create background models.

Before the start of the inversion, based on the calculation of synthetic traces, the correlation of well-logging data with seismic migrated cross-sections was performed.

The input data for this inversion are the background velocity models for longitudinal and transverse waves and density, created by krigging- interpolation of borehole curves along the frame, defined by the surfaces of the reflecting horizons.

The main requirement for the background model is the construction of such a volumetric model which has no anomalies due to the poor quality of the well-logging in individual intervals of the cross - section. It should reflect the geological view of the cross - section structure. Models were created in the deep window from 1000 to 3500 m. In order to build a background model in the layers, the following wells were used: SGK-03, SGK-04, SGK-06, SGK-07, SGK-08, SGK-09.

For inversion 3 models were created: longitudinal and transverse wave velocities and densities, which, together with the CDP seismograms after deep migration, the impulse determined during the calculation of synthetics, were fed to the inversion input (fig. 5.6). Synthetics calculation was performed for all wells.

The result of the inversion is illustrated in the figure (fig. 5.7). Cubes of P-impedance, S-impedance, and density were obtained. According to the impedance values, it is possible to divide the cross-section into complexes with close values of physical parameters, allocating relatively thin layers in them that correspond to relative impedance fluctuations.

After seismic inversion, a comparison of the log data (well-logging) and the downloaded seismic data was done: P-impedance, S- impedance and densities from all wells (fig. 5.8 – 5.9).

The impedance cube was converted into the effective porosity cube by the cubic dependence found from the cross-plot between the porosity curves and impedance curves in wells SGK-03, SGK-04, SGK-07, SGK-09 (fig. 5.10). High impedance values correspond to the low porosity values and vice versa (fig. 5.11). Figures 5.12 - 5.14 illustrate porosity maps of reflecting horizons.

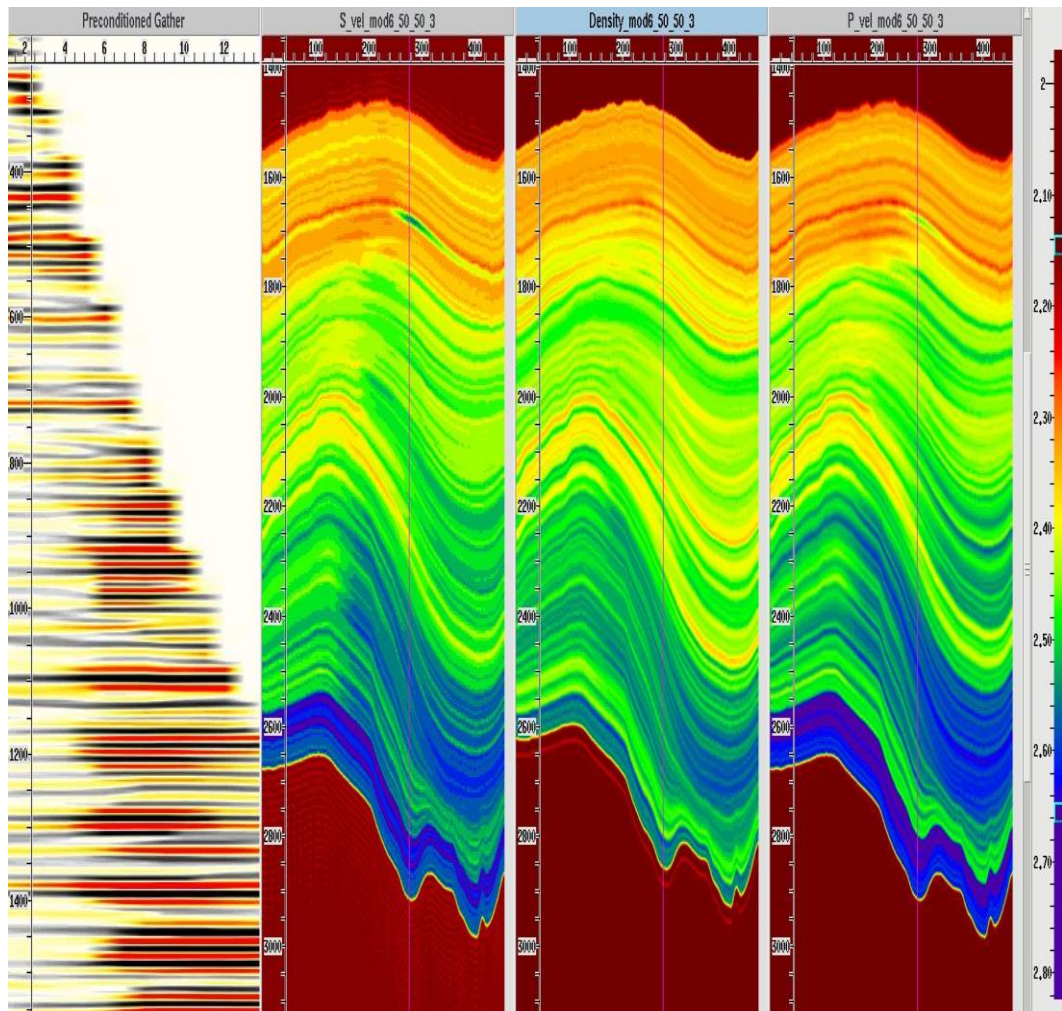


Figure 5.6 – Input data for inversion: seismogram CDP (a), transverse wave velocity (b), density (c) and longitudinal wave velocity (d)

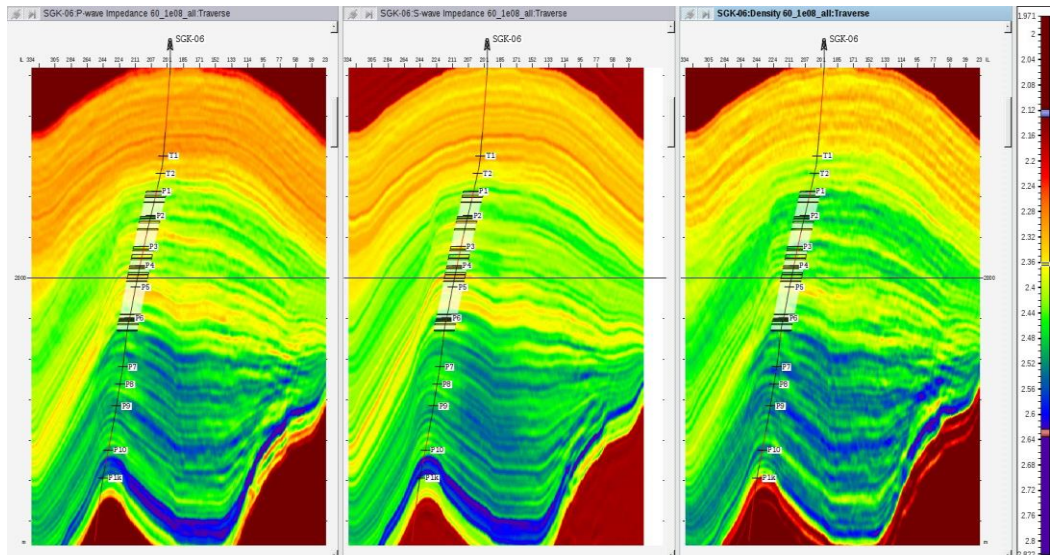


Figure 5.7 – Cross-section of the longitudinal wave impedance (a), transverse wave impedance (b) and density (c)

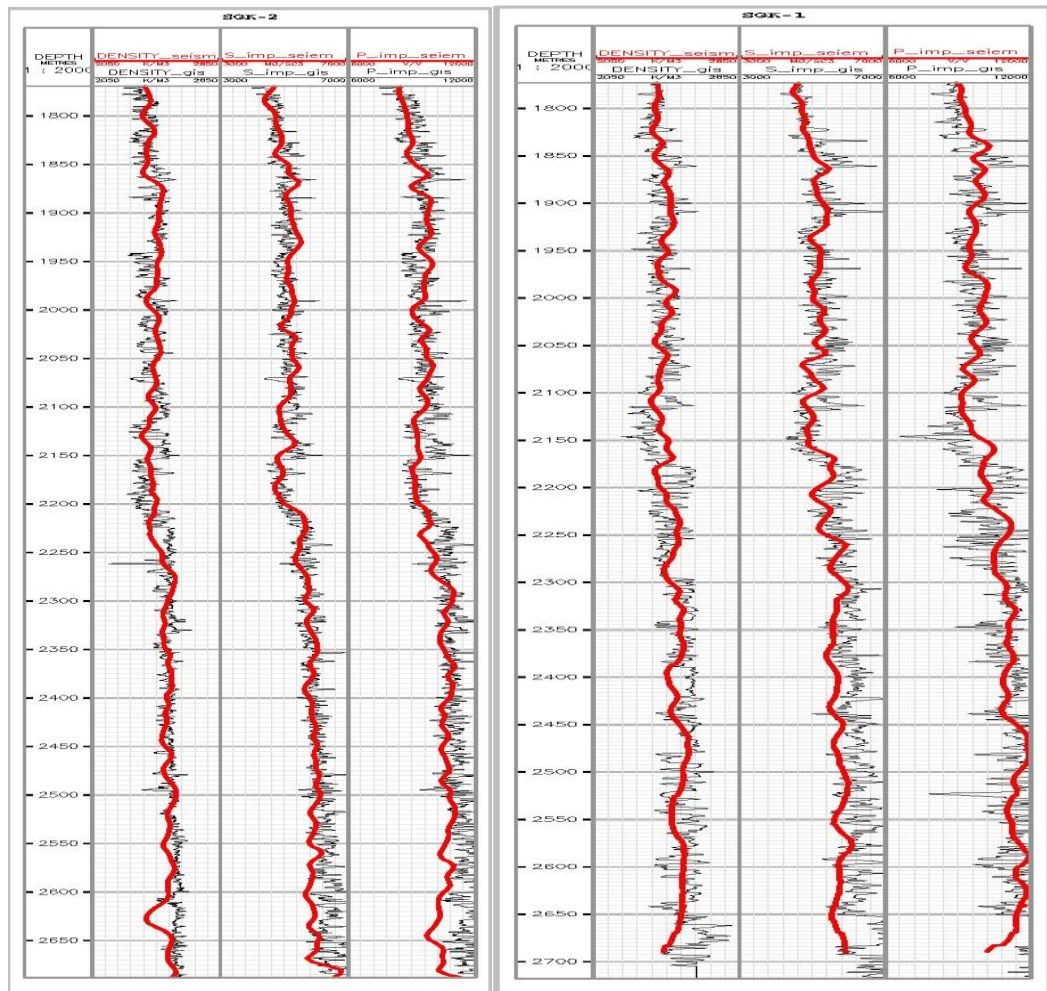


Figure 5.8 – Comparison of well-logging data and seismic data: P-impedance, S-impedance and densities of the wells SGK-01 and SGK-02

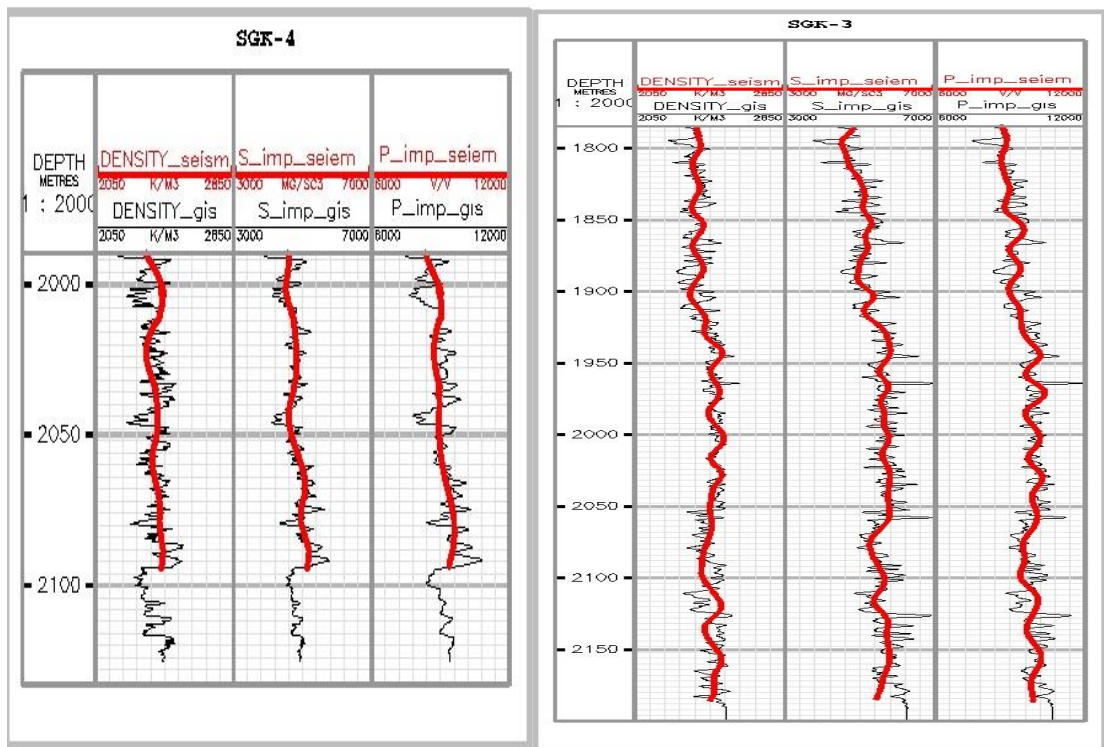


Figure 5.9 – Comparison of well-logging data and seismic data: P-impedance, S-impedance and densities of the wells SGK-03 and SGK-04

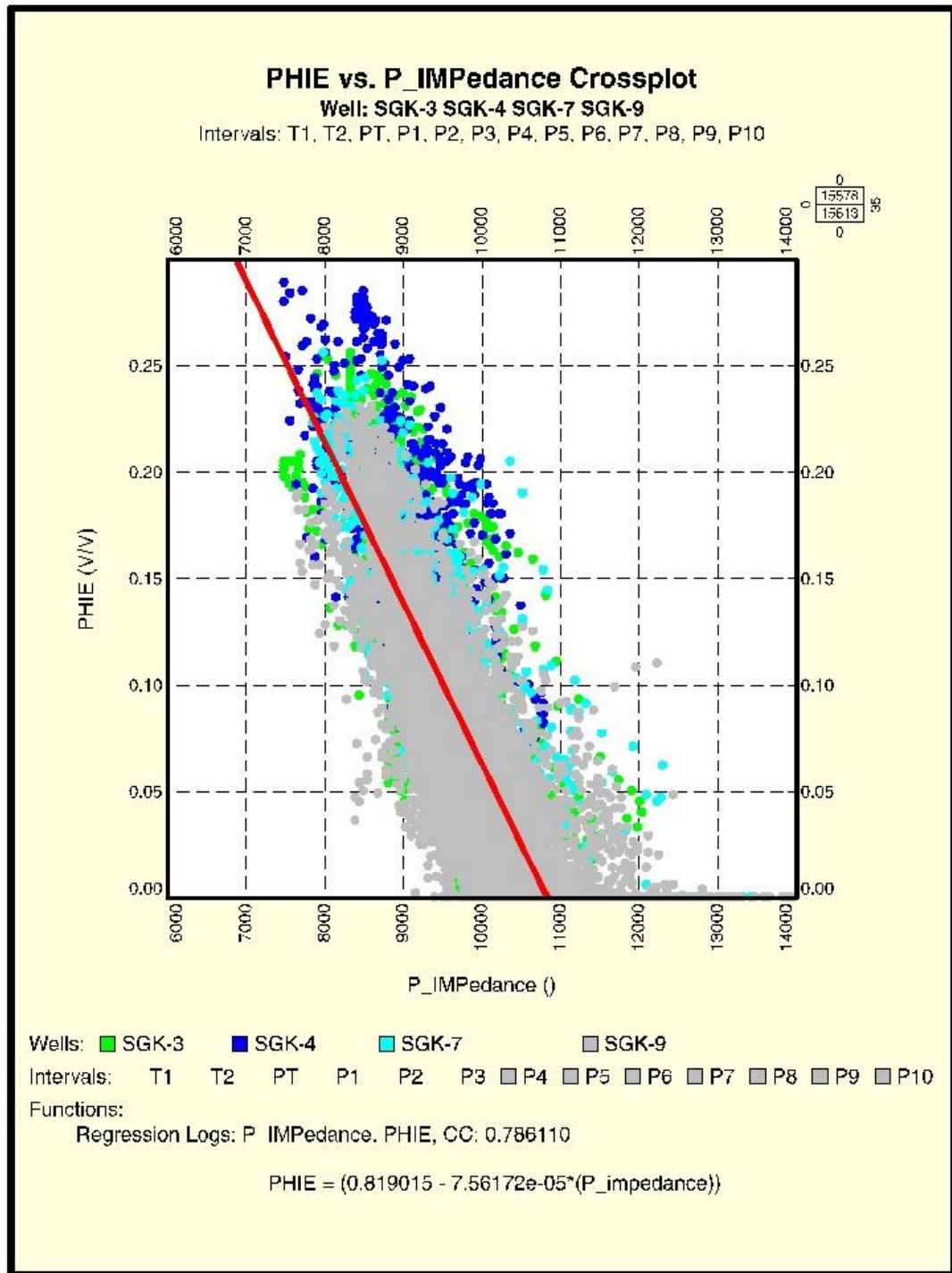


Figure 5.10 – Dependence of porosity according to well-logging data (PHIE) and acoustic stiffness (P-impedance)

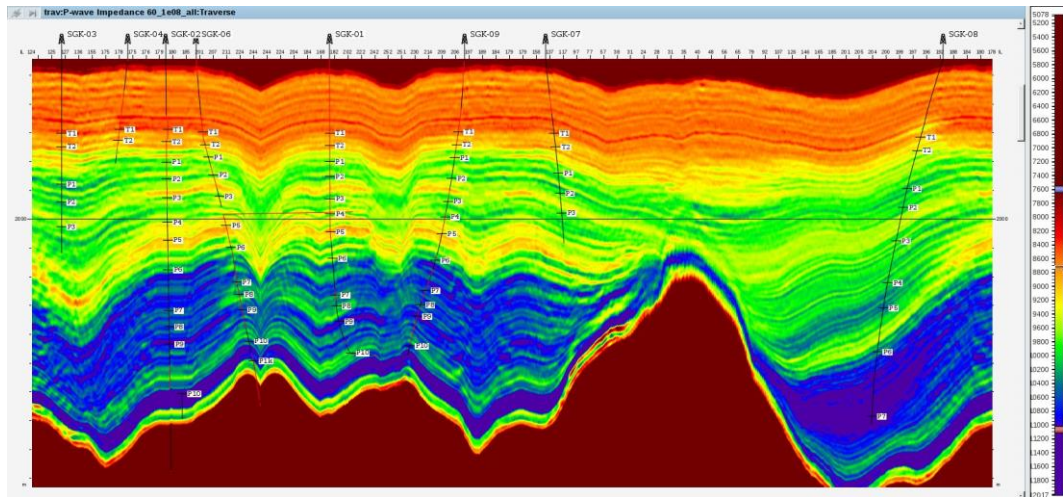
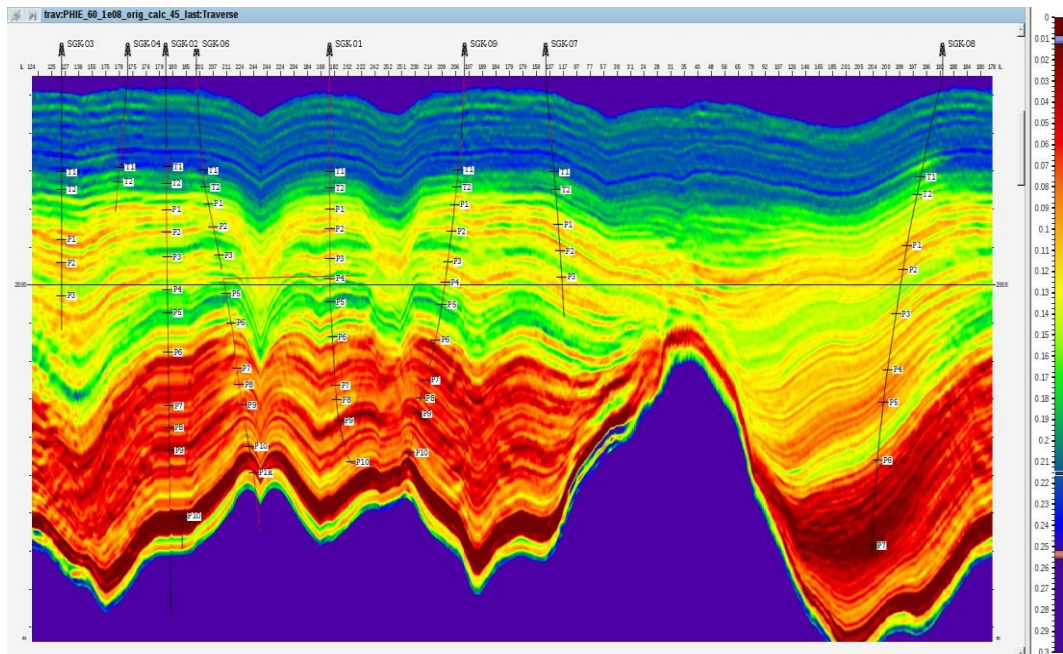


Figure 5.11 – (a) Acoustic stiffness cross-section (P-impedance), (b) porosity cross-section (PHIE), along the traverse line



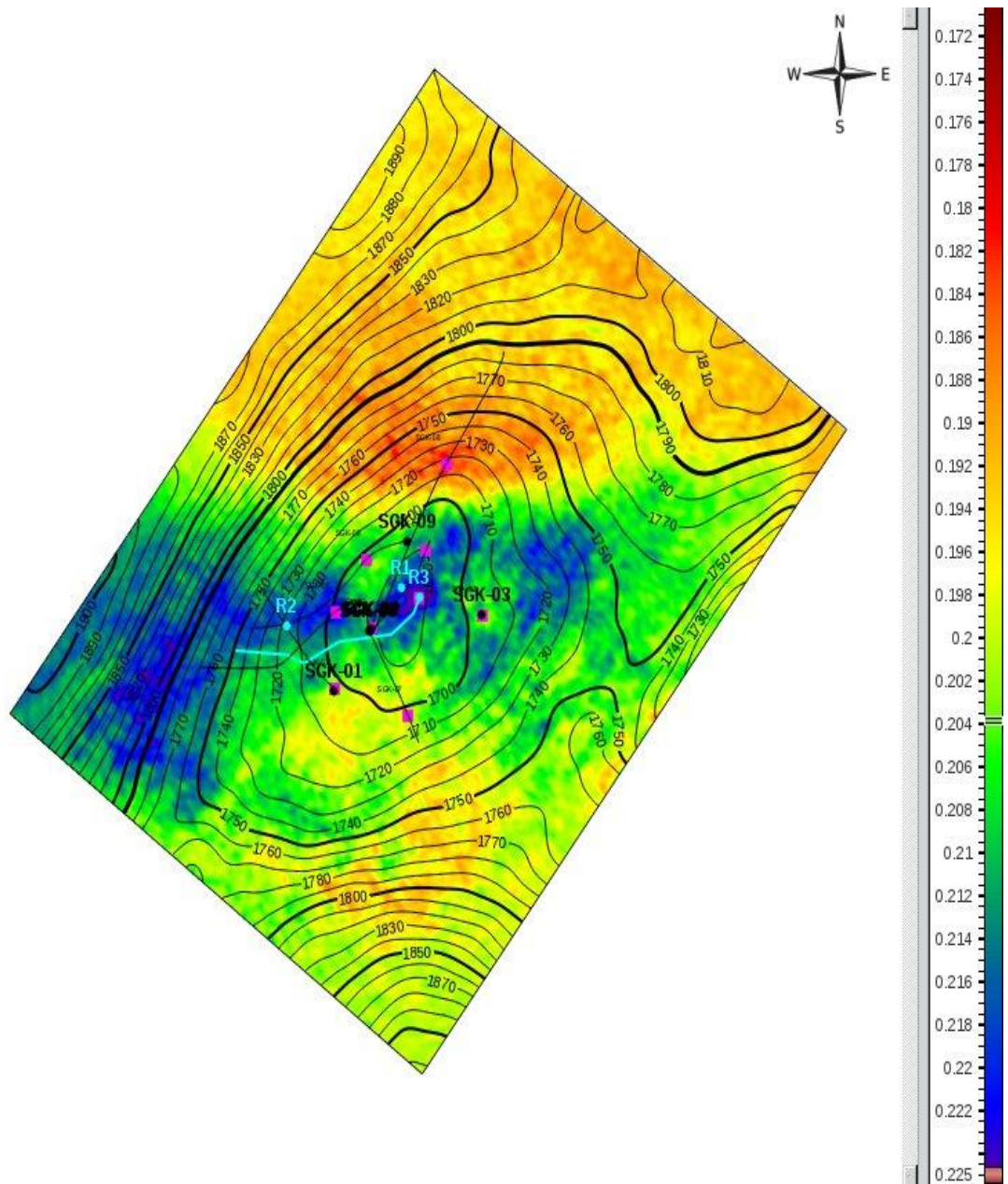


Figure 5.12 – Map of porosity (PHIE) for the reflecting horizon T1

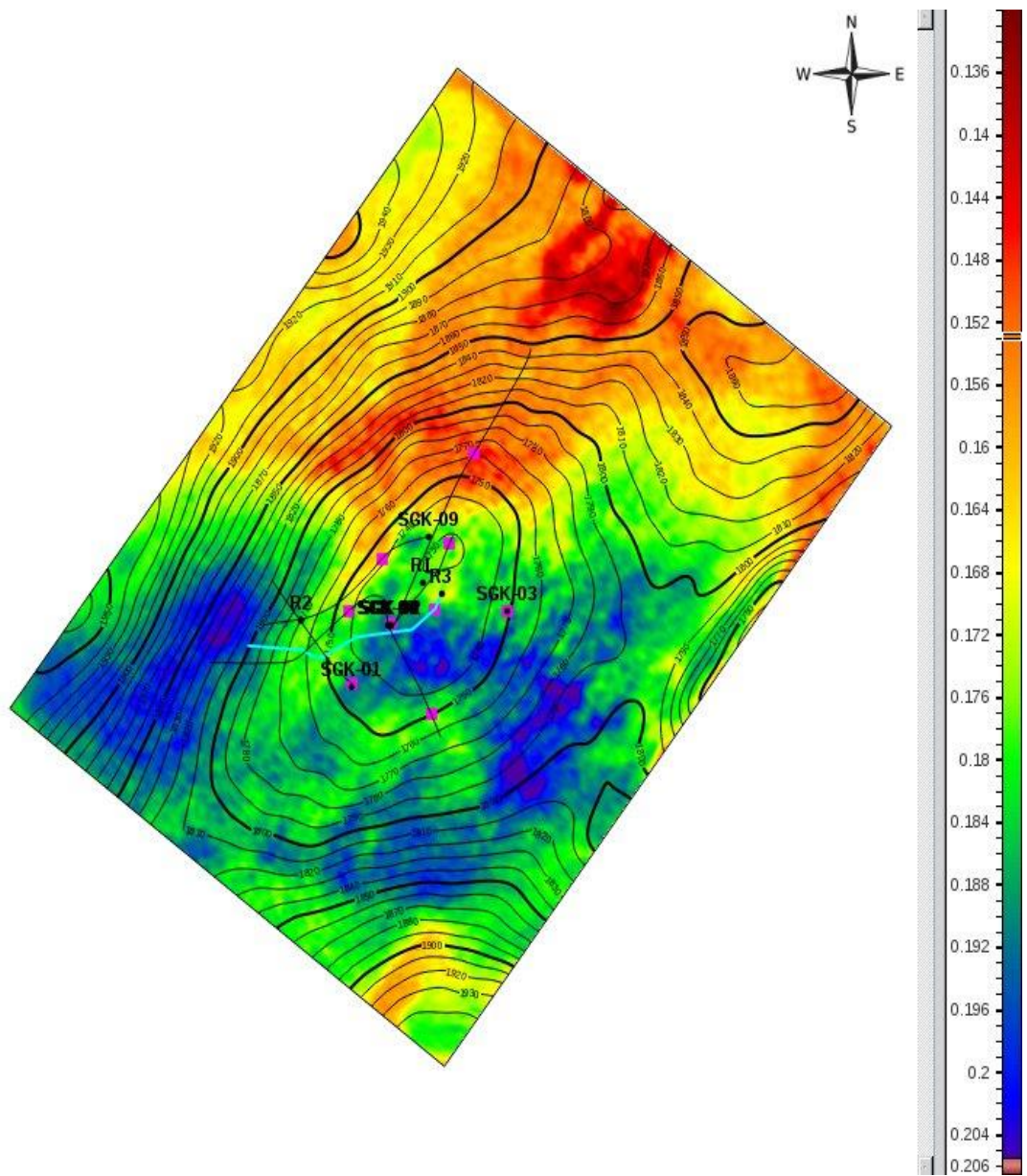


Figure 5.13 – Map of porosity (PHIE) for the reflecting horizon T2

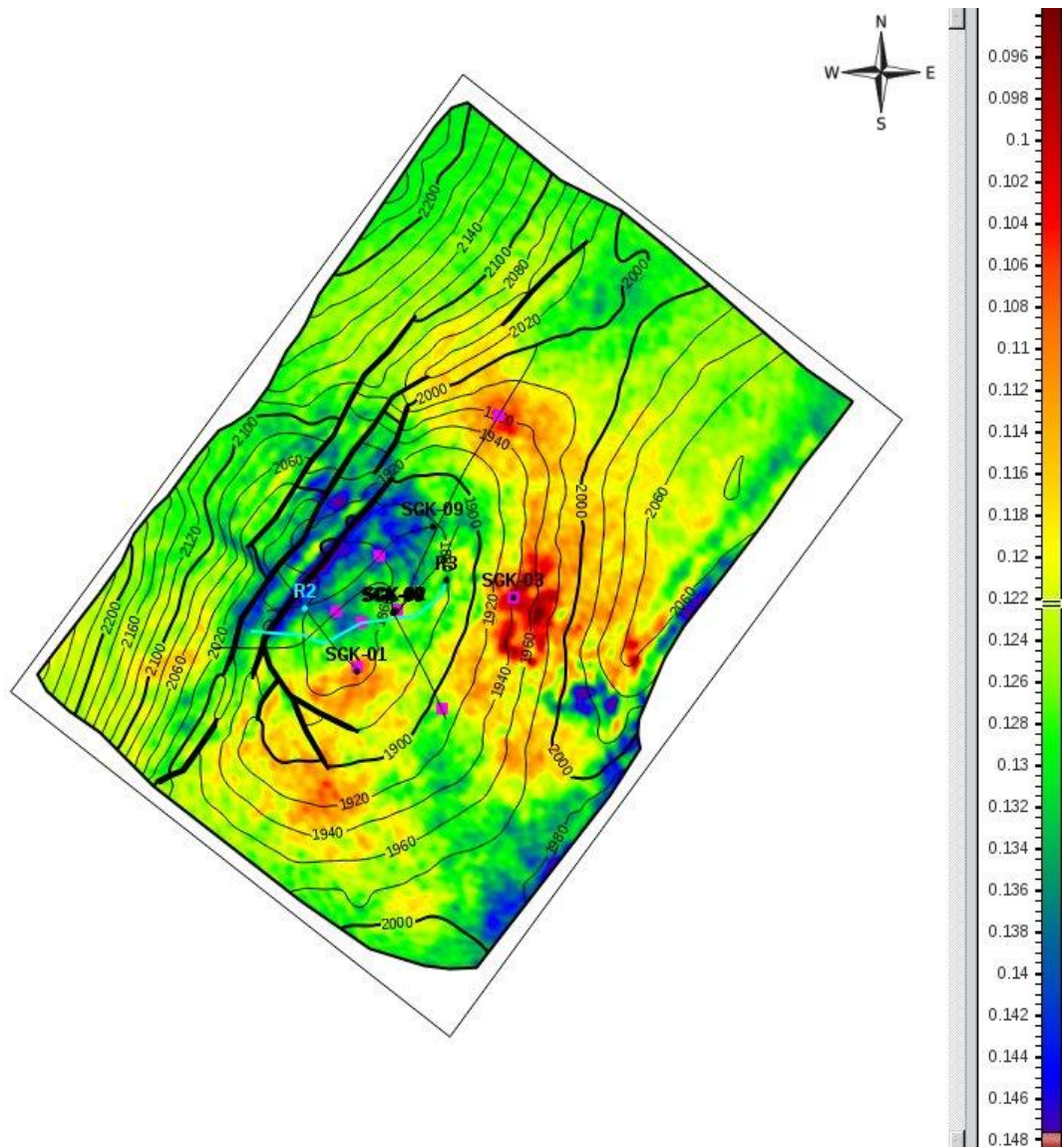


Figure 5.14 – Map of porosity (PHIE) for the reflecting horizon P2

5.4 Coherence

Coherence is calculated over a deep seismic cube. Coherence makes it possible to outline and visualize inhomogeneities in the wave field, such as faults (both low-amplitude and large), fracture zones, buried channels, and etc. In turn, areas with a good signal are accompanied by maximum coherence. Such coherence properties make it possible to additionally analyze the wave field and help with interpretation not only in difficult geological conditions, but can be also useful in interpreting seismic data from a relatively calm geological situation. During the calculation of coherence, evaluation of signal continuity is obtained from a set of seismic traces, and is used directly or indirectly. The result of coherence calculation is highly

dependent on the quality of the material. Zones of high coherence in sections and cross-sections are usually highlighted by a bright field (in a black-white palette).

Figures 5.15-5.16 illustrate examples of sections along the horizons and are compared with structural maps. Fracture zones and heterogeneity zones are clearly visible on the sections.

The data from the results of coherence analysis are in good agreement with the results of the prediction of porosity and were taken into account when determining the positions of exploratory wells.

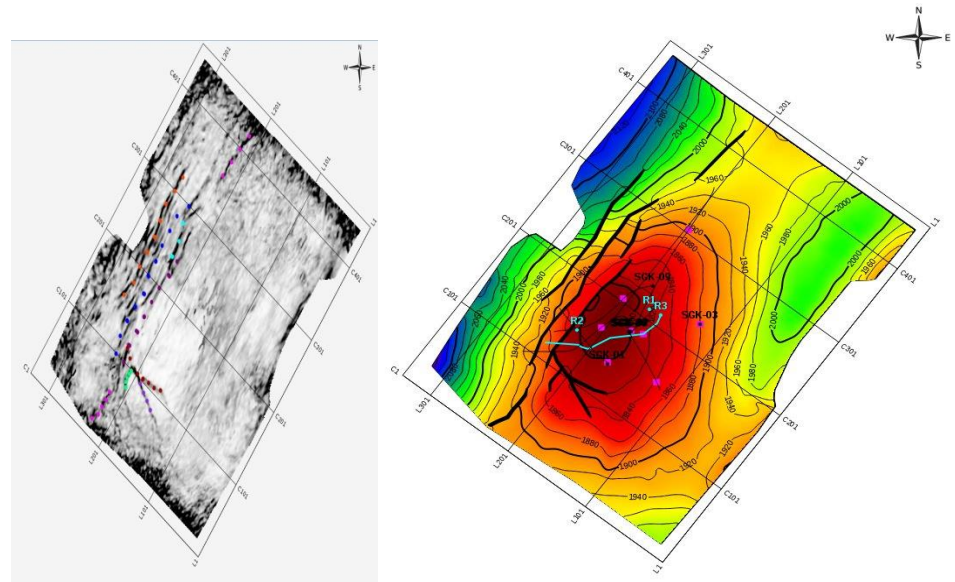


Figure 5.15 – Coherence (on the left) and structural plan (on the right) of the P1 horizon

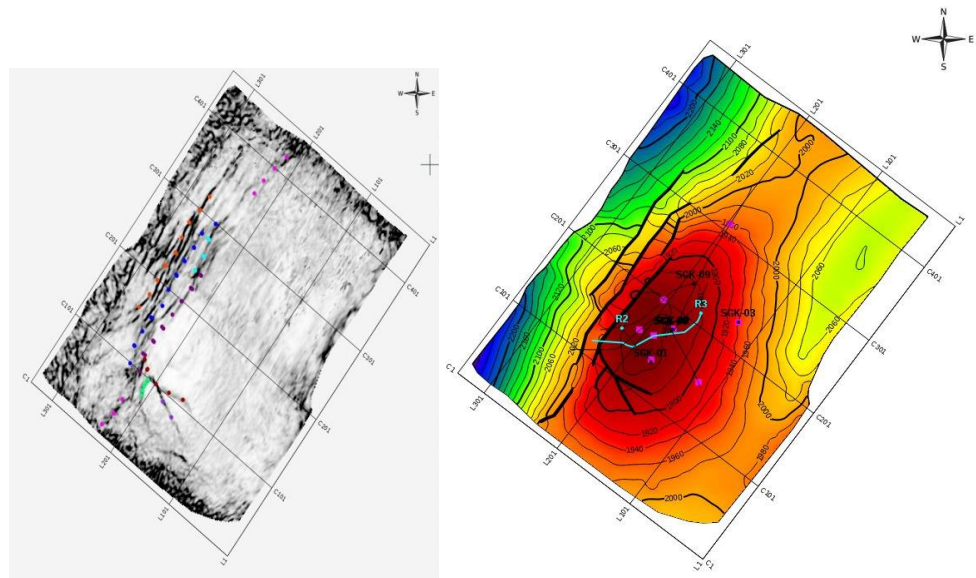


Figure 5.16 – Coherence (on the left) and structural plan (on the right) of the P2 horizon

5.5 Seismic-facial analysis

During the conduction of seismic-facial analysis, the “Stratimagic” program was used. This program performs an automatic classification and interpretation of seismic facies by the waveform using neural network technology.

Seismic facies combine a group of reflections characterized by a similar set of parameters, such as configuration, continuity, amplitude, frequency and etc. Each parameter carries certain information about the geological structure of the studied interval. The configuration of the reflections is closely related to the main characteristics of the bedding, the continuity of reflections with the continuity of the layers, the amplitude shows the ratio of density and velocity, the frequency depends on the thickness of the layers, and etc.

At the first stage, horizon correlation was carried out. In the second stage, which involves the selection method, were calculated seismic facies in the interval of the reflecting horizons T1-P10. The wave field was divided from 6 to 14 seismic facies. Over all horizons, values of seismic facies were extracted and maps were constructed (figure 5.17 – 5.19). Different colours of facies indicate a change in the wave field.

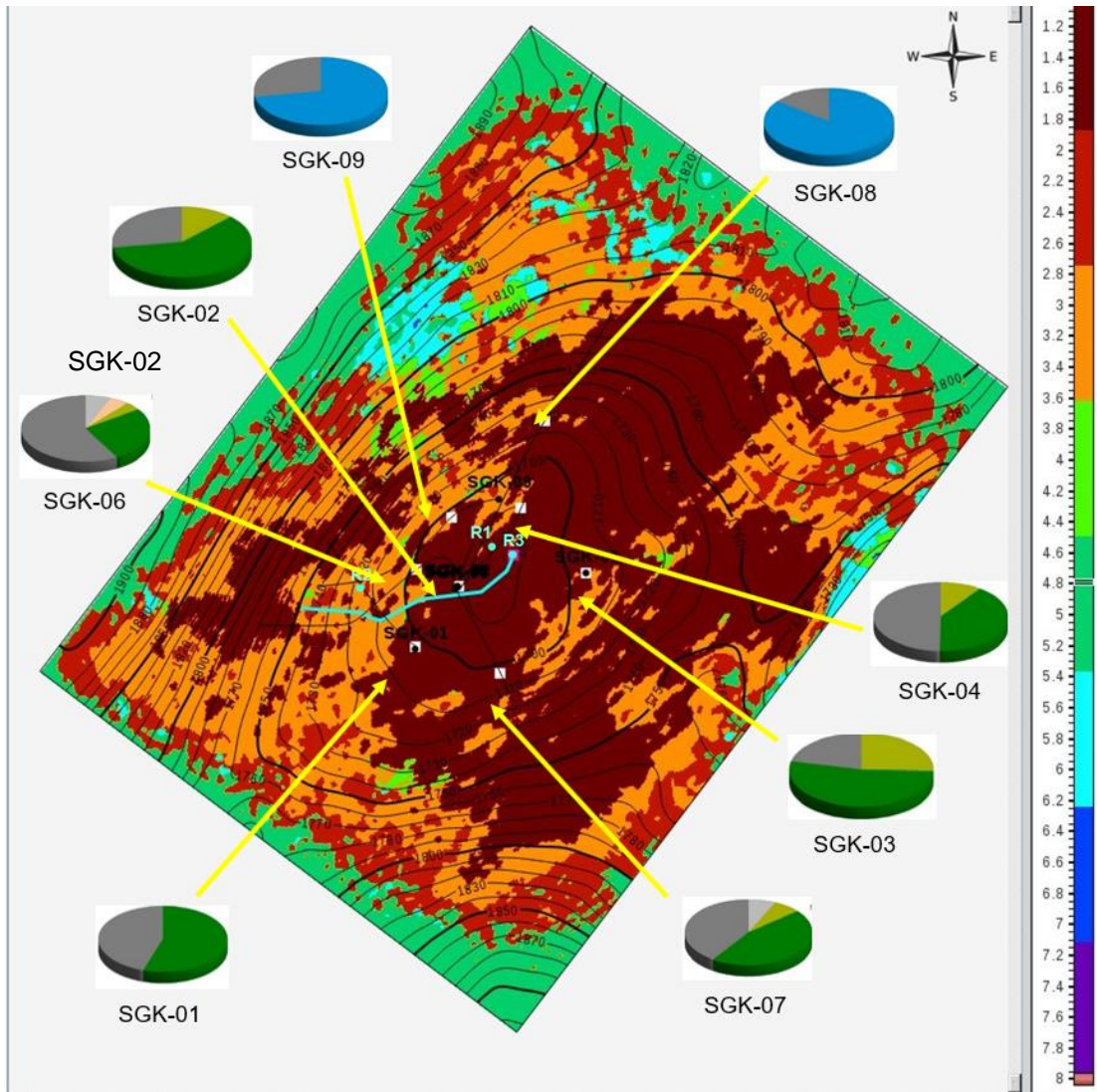


Figure 5.17 – Seismic Facial Analysis of T1 horizon

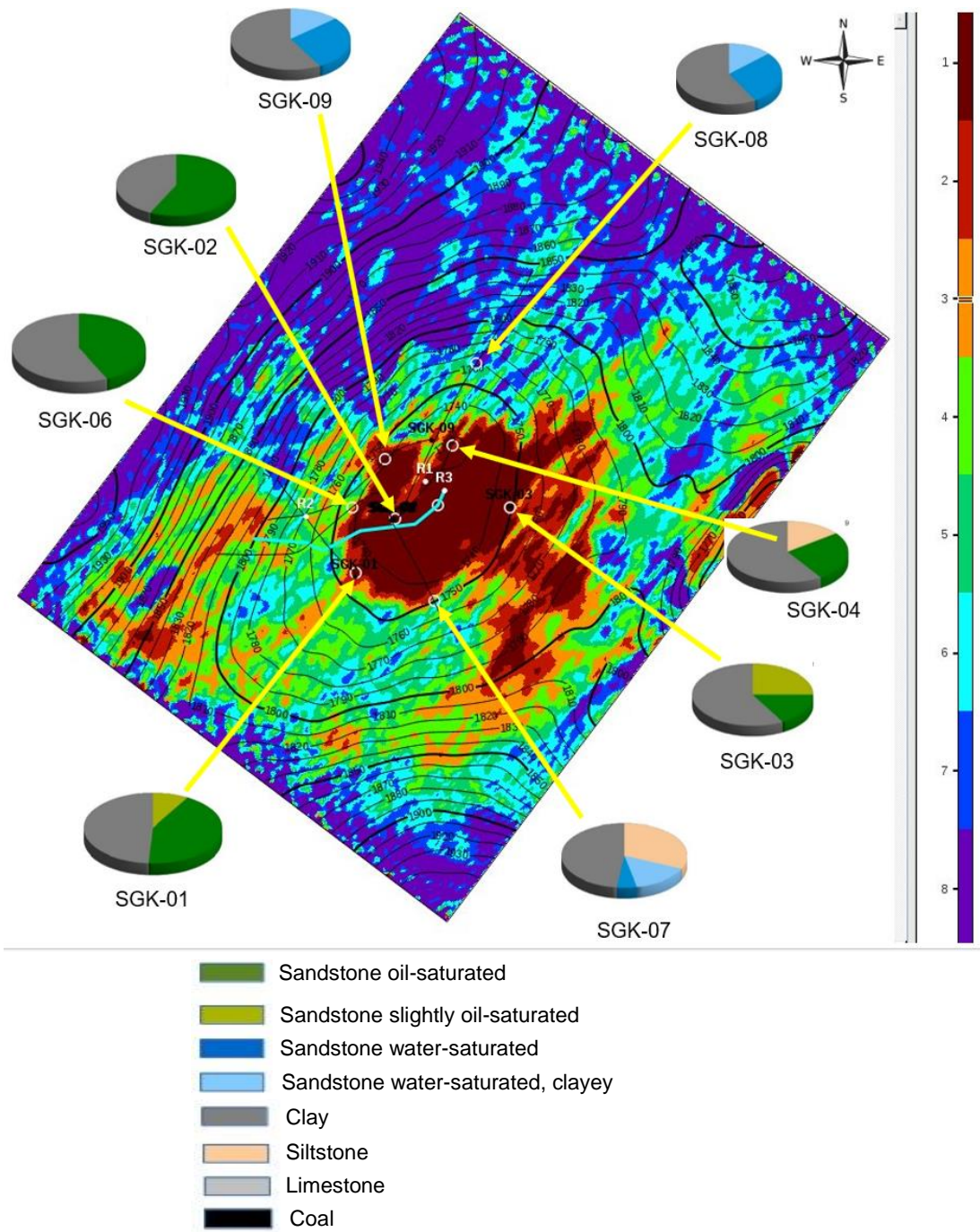


Figure 5.18 – Seismic Facial Analysis of T2 horizon

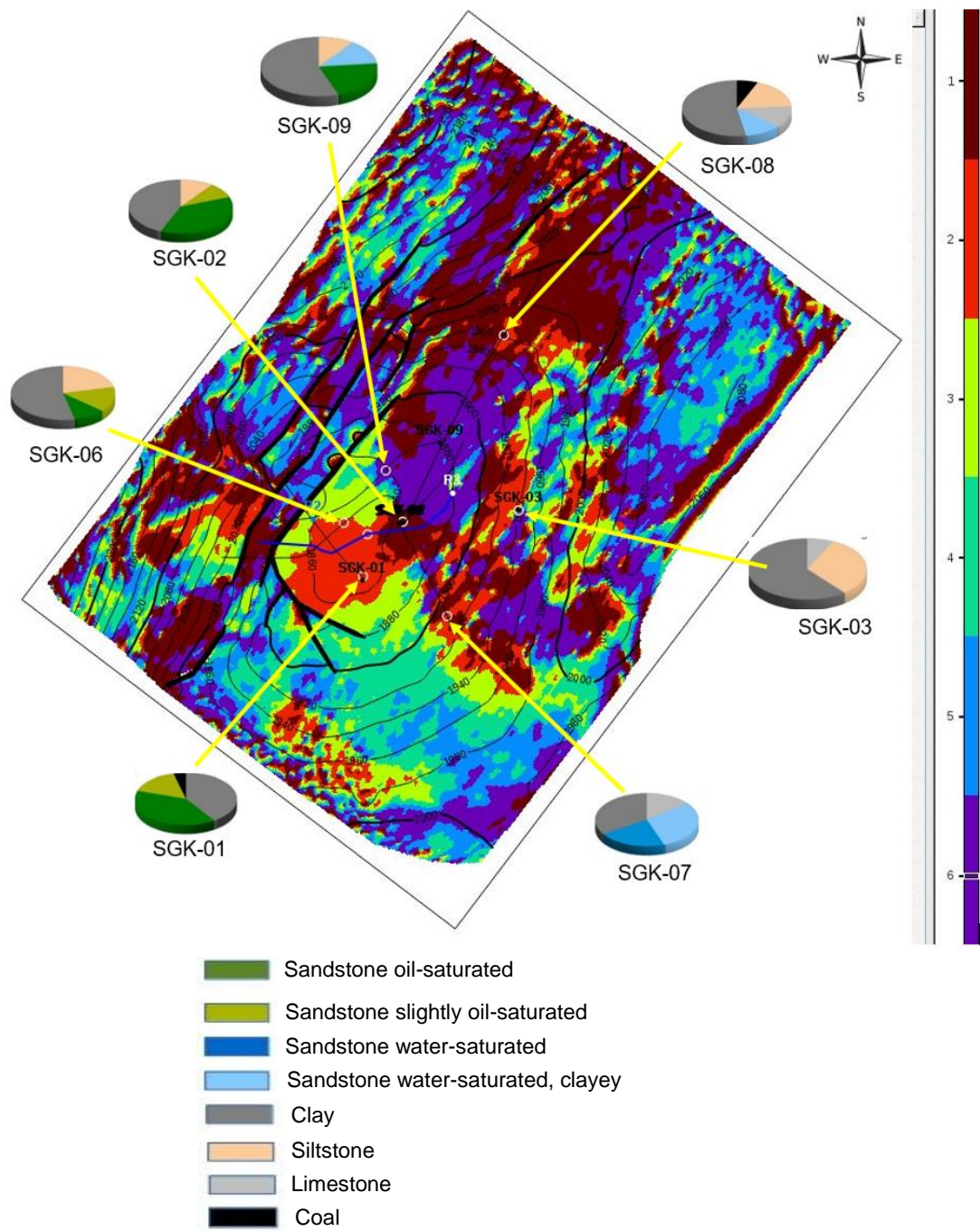


Figure 5.19 – Seismic Facial Analysis of P2 horizon

6 Analysis of dynamic interpretation results

After the conduction of the main stages of interpretation, an analysis of dynamic methods was made, the features of their application for studying Permian sediments were considered.

Seismic inversion

The most informative method is the seismic inversion. Good results were obtained due to the high-quality reprocessing of 3D seismic data and reinterpretation of the logging data. When processing seismic data, the true amplitude-frequency characteristics of the signal were constantly monitored, which allowed us to achieve high values of the correlation of seismic and well-logging data. Based on the obtained 3D seismic inversion cube, porosity maps were constructed for all productive horizons.

On the obtained maps of porosity along the T1 horizon (sediments of the Middle Triassic), it can be seen that the values of porosity within the reservoir vary slightly, from 20 to 22%. The reservoir is sustained, the lithological composition of the rocks is homogeneous (Figure 6.1). It can be seen that the best reservoirs are located in the suite part of the structure.

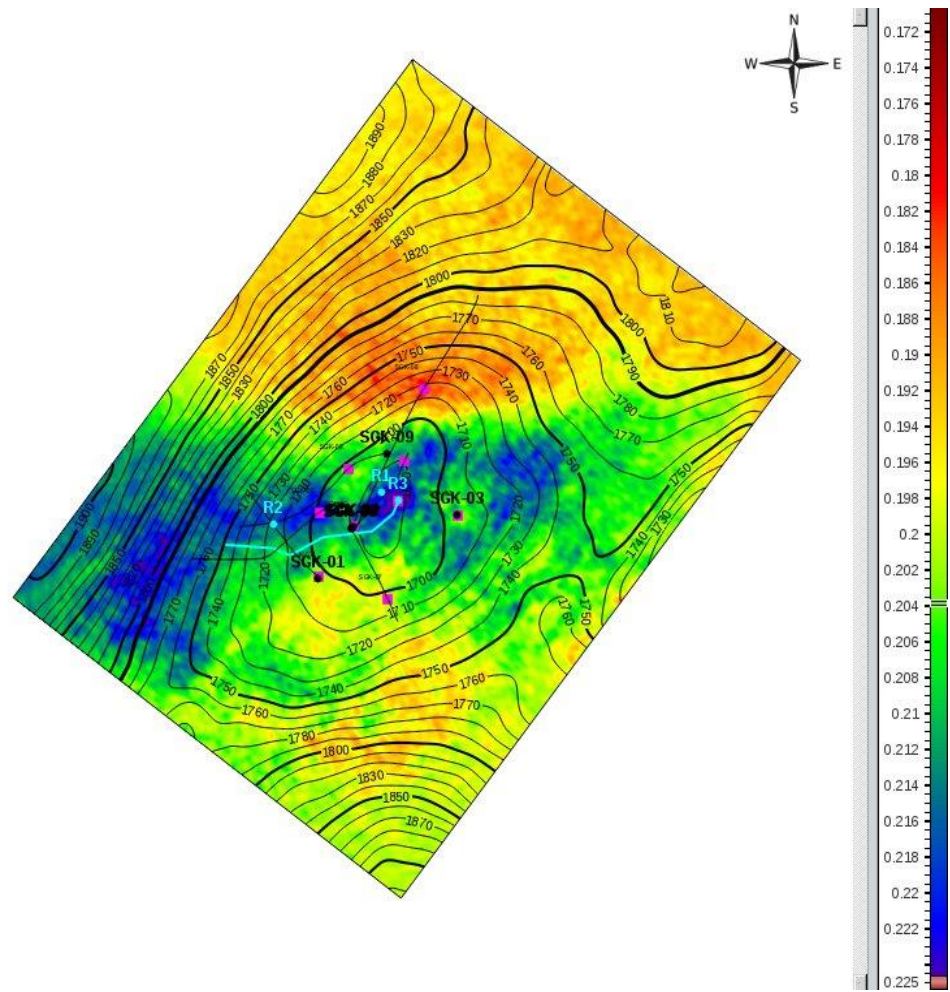


Figure 6.1 – Map of porosity (PHIE) for reflecting horizon T1

On the map of porosity along the P2 horizon (sediments of the Tatarian stage of the Upper Permian), we are able to see that the maximum values of porosity are located in the northern and northwestern parts of the structure, in the suite part the reservoir properties were noticed to be deteriorated, and on the southern wing of the structure porosity decreases to critical values (Figure 6.2). This feature is visible on almost all Permian horizons. Because of the seismic inversion, it is now possible to confidently say that reservoirs in Permian sediments are very different from Triassic reservoirs not only in porosity, but also in the homogeneity of the composition of the host rocks.

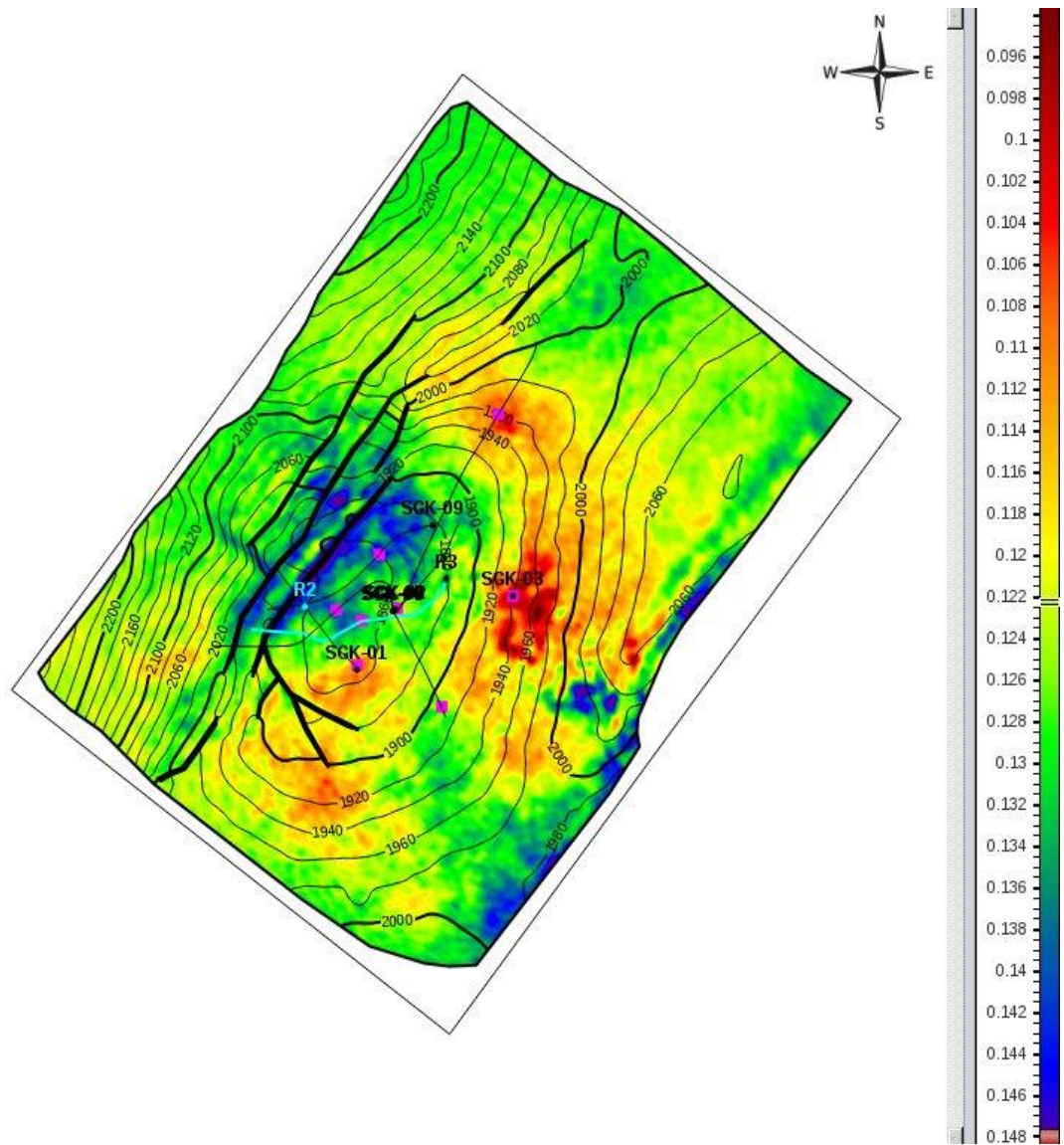


Figure 6.2 – Map of porosity (PHIE) for reflecting horizon P2

Seismic-facial analysis

The second most important method when conducting dynamic interpretation is the seismic-facial analysis. This method allows to predict the lithological composition of sedimentary deposits.

When conducting the seismic-facial analysis, the "Stratimagic" program was used. This program automatically classifies and interprets seismic facies by waveform using neural network technology.

Were calculated seismic facies in the interval of reflecting horizons T1-P10. The wave field was divided from 6 to 14 seismic facies. Across all horizons, seismic facies values were extracted and maps constructed.

Analyzing the seismic facies along the T1 horizon (sediments of the Middle Triassic), we see that only two seismic facies are distinguished within the structure.

This allows to assume that the lithological composition of the rocks is relatively homogenous.

At the same time, seismic-facial analysis along the P2 horizon (Permian sediments) highlights six seismic facies within the structural plan (Figure 6.4). The lithological composition of the sediments is heterogeneous; reservoir properties can vary over a wide range.

The differences between the Triassic and Permian seismic facies allows to say that the sedimentation process of Permian sediments was more complex, with intense tectonic impact and frequent changes in climatic conditions. As a rule, under such conditions, the formation of stratigraphically and lithologically shielded deposits is possible.

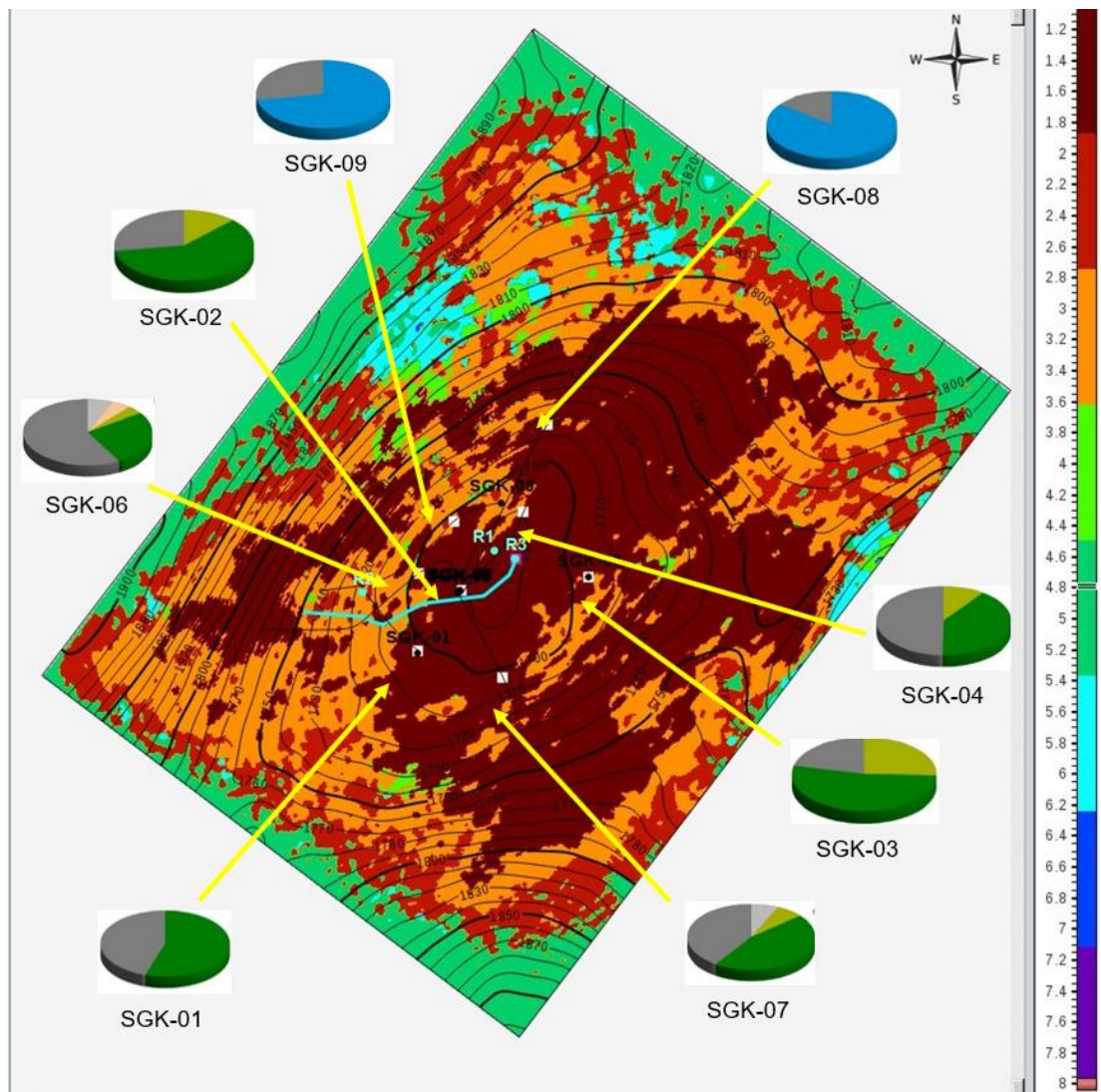


Figure 6.3 – Analysis of seismic facies by horizon T1

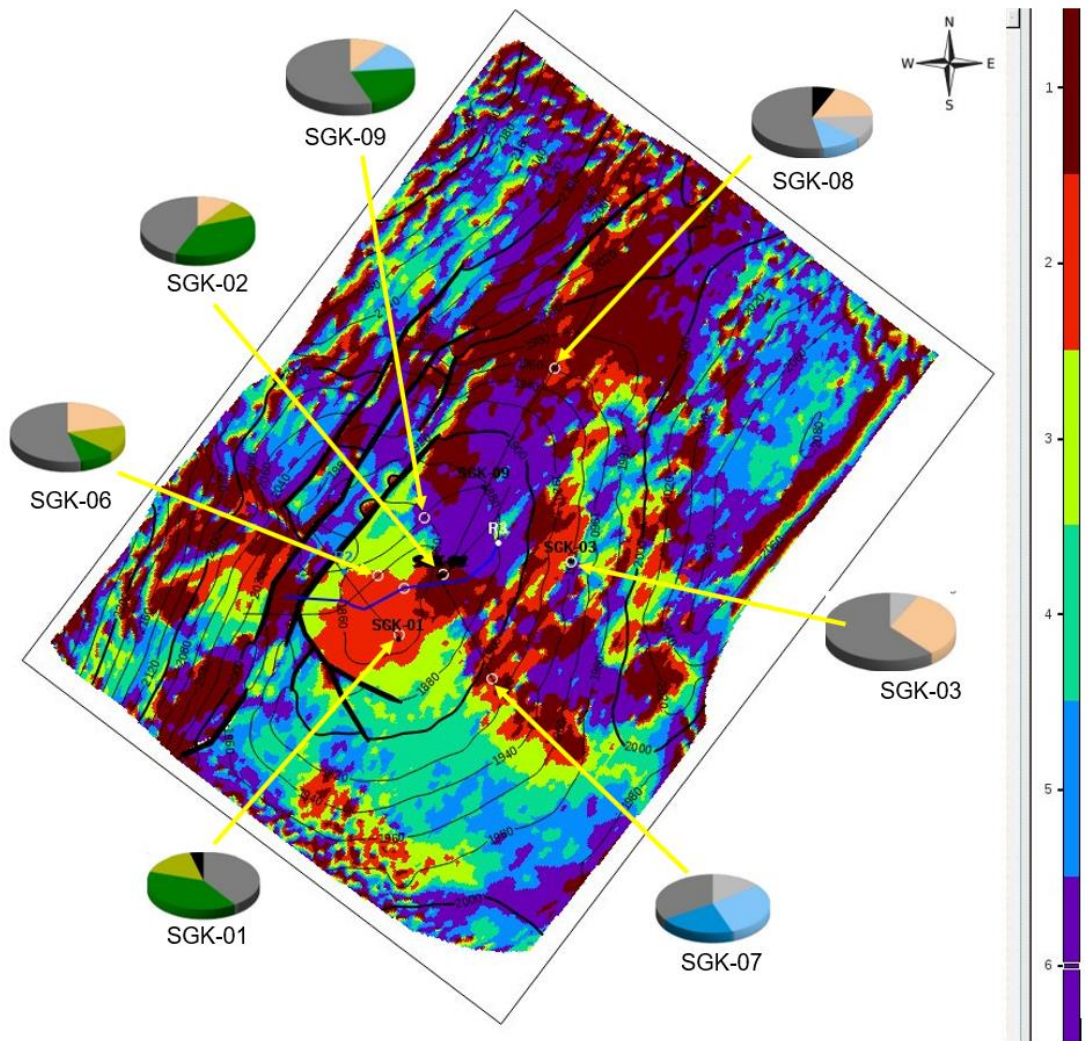


Figure 6.4 – Analysis of seismic facies by horizon P2

Coherence

Coherence is calculated according to a deep seismic cube. Coherence makes it possible to highlight and visualize inhomogeneities in the wave field, such as faults (both low-amplitude and large), fracture zones, buried channels and etc.

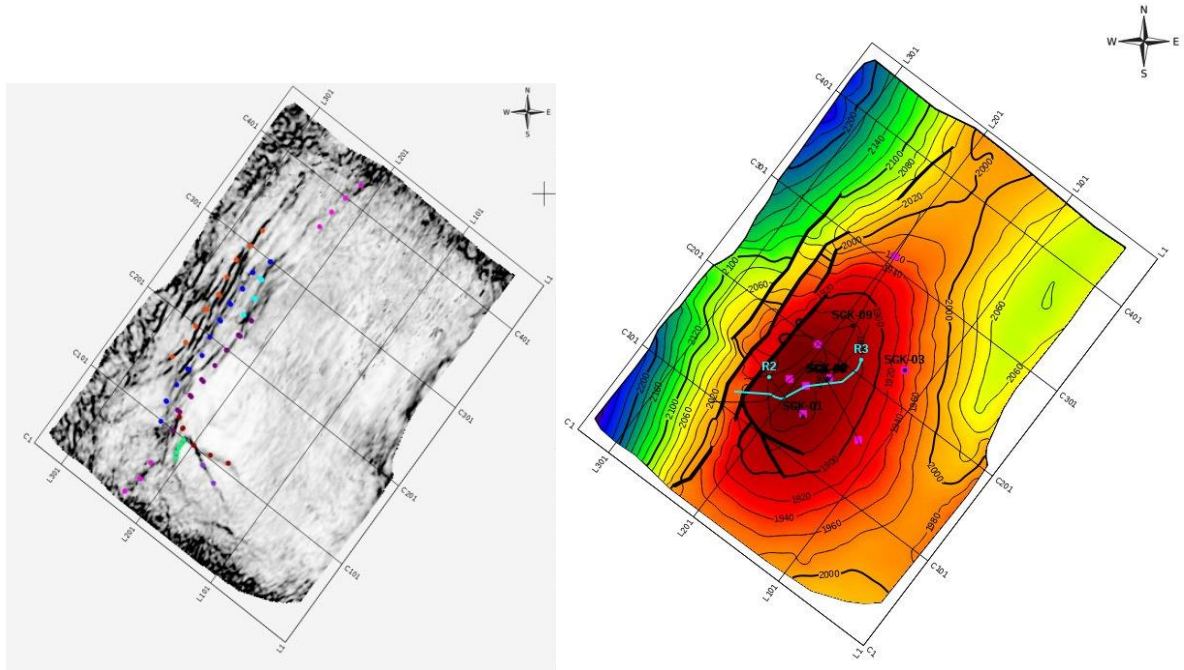


Figure 6.5 – Coherence and structural plan for horizon P2

On the Figure 6.5 is illustrated a horizontal cut of the coherence cube (on the left) and a structural map along the horizon P2. It can be seen that tectonic disturbances on the western wing of the structure are correlating with highlighted inhomogeneities on the coherence cut. Unfortunately, it was not possible to highlight the zones of fracture and paleochannels.

CONCLUSION

In this diploma work, was considered the possibility of modern dynamic interpretation methods for studying Permian-Triassic deposits. Thanks to the industrial practice in the "Saigak Kazakhstan B.V." company, I was able to trace in detail the entire processing and interpretation process at the Saigak deposit, where the target was Permian and Triassic sediments.

As a result of the analysis of the obtained dynamic interpretation data, the following conclusions can be drawn:

Permian and Triassic sediments were forming under various conditions of sedimentation. If the Triassic sediments are lithologically sustained, the basic characteristics of rocks, such as density, porosity and permeability, are practically constant within the reservoir, then Permian sediments are lithologically and stratigraphically not sustained. Without the dynamic analysis, it is impossible to highlight the zones of lithological substitution. The porosity values vary over a very wide range, there are local zones of secondary porosity development (fractured reservoirs), lithologically shielded deposits may be highlighted.

Successful drilling requires a prediction of promising areas. The quality of the dynamic interpretation depends on the quality of the performed field work. Unfortunately, according to the regional data (2D seismic), such work is impossible. It is necessary to conduct high-frequency 3D seismic, use high-quality logging, especially density and acoustic methods, to conduct an accurate core analysis.

At the present time in Kazakhstan there is a large number of deposits, where exploration and production are carried out in Permian-Triassic sediments. The application of dynamic interpretation methods will allow to achieve good results during the conduction of exploration works.

LIST OF REFERENCES

- 1 Avrov V.P., Bulekbayev Z.Y., Daumov S.G., Kraev P.I. «Prospects for the oil and gas potential of the south-eastern side of the Caspian depression», Vestnik AS Kaz. SSR, №2, 1960 y.
- 2 Daukeev S.Z., Vozalevskiy E.S., Pilifosov V.M. «The deep structure and mineral resources of Kazakhstan», Oil and gas, volume III, Almaty, 2002 y.
- 3 Dahnov V.N. «Interpretation of the results of geophysical surveys of wells», M., Nedra, 1977 y.
- 4 Latypova M.G., Martynov V.G., Sokolova T.F. «Well-logging Interpretation Practical Guide», M., Nedra, 2007 y.